The Plant Cell, Vol. 4, 1383–1404, November 1992 © 1992 American Society of Plant Physiologists

Regional and Cell-Specific Gene Expression Patterns during Petal Development

Gary N. Drews,[1] Thomas P. Beals, Anhthu Q. Bui,[2] and Robert B. Goldberg[3]

Department of Biology, University of California, Los Angeles, California 90024-1606

We investigated gene expression patterns that occur during tobacco petal development. Two petal mRNA classes were identified that are present at elevated levels relative to other organs. One class is represented equally in the unpigmented tube and pigmented limb regions of the corolla. The other class accumulates preferentially within the limb region. Limb-specific mRNAs accumulate at different times during corolla development, peak in prevalence prior to flower opening, and are localized in either the epidermal cell layers or the mesophyll. The epidermal- and mesophyll-specific mRNAs change abruptly in concentration within a narrow zone of the limb/tube border. Preferential accumulation of at least one limb-specific mRNA occurs within the corolla upper region early in development prior to limb maturation and pigment accumulation. Limb-specific mRNAs also accumulate preferentially within the unpigmented corolla limb region of *Nicotiana sylvestris*, a diploid progenitor of tobacco. Runoff transcription studies and experiments with chimeric β-glucuronidase genes showed that petal gene organ, cell, and region specificities are controlled primarily at the transcriptional level. We conclude that during corolla development transcriptional processes act coordinately on limb-specific genes to regulate their regional expression patterns, but act individually on these genes to define their cell specificities.

INTRODUCTION

The petal is one of two nonreproductive organs of the flower (Esau, 1977; Raven et al., 1986). This organ serves to protect the floral reproductive organs and to attract pollinators to ensure that pollination and fertilization occur (Raven et al., 1986). The petal develops from primordia that are initiated on the floral meristem during the early stages of flowering (Hicks, 1973; Esau, 1977; Drews and Goldberg, 1989; Smyth et al., 1990). At least two homeotic genes, thought to encode transcriptional activator proteins, direct specific floral primordia to follow a petal differentiation pathway (Schwarz-Sommer et al., 1990; Coen, 1991; Coen and Meyerowitz, 1991). The processes responsible for activating homeotic genes that control petal differentiation within specific meristem domains are not known. Nor is it known how cell types are specified during petal development, how tissue organization patterns are established following petal primordia specification, what elaborates petal shapes, or how petals fuse within the corolla.

Previously, we employed RNA-excess DNA/RNA hybridization studies with single-copy DNA to show that there are approximately 25,000 diverse genes expressed within the tobacco petal (Kamalay and Goldberg, 1980, 1984). Hybridization experiments using a subtracted single-copy DNA probe, representing genes expressed in the leaf, indicated that genes active in the petal are indistinguishable from those expressed in the leaf, within the resolution of the procedure (Kamalay and Goldberg, 1980). Comparisons with other organ system mRNAs indicated, however, that the petal/leaf gene set contains approximately 6000 diverse genes that are not expressed in other organs (Kamalay and Goldberg, 1980). These results indicate that the analogous differentiated states of the petal and leaf correlate with the expression of similar gene sets, and that differential gene expression is required to specify individual cell types during the development of these organs. Recently, others have used anthocyanin and amino acid biosynthesis genes to show that gene expression is regulated with respect to both region and cell type within the petal (Benfey and Chua, 1989; Koes et al., 1990; Jackson et al., 1992), and have identified putative transcriptional control genes that operate during petal development (Goodrich et al., 1992; Takatsuji et al., 1992).

In this paper, we describe the expression patterns for several tobacco genes that are expressed at elevated levels in the petal relative to other organs. We identified two petal mRNA sets—one that is represented equally in the unpigmented tube and pigmented limb regions of the corolla, and another that accumulates preferentially within the pigmented limb region. Limb-specific mRNAs accumulate with different temporal kinetics during corolla development, are localized in either the epidermal cell layers or the mesophyll, and drop precipitously in concentration within a narrow zone of the tube/limb region. Preferential accumulation of limb-specific mRNAs occurs prior

[1] Current address: Department of Biology, University of Utah, Salt Lake City, UT 84112.

[2] Current address: Department of Botany, University of California, Davis, CA 95616.

[3] To whom correspondence should be addressed.

to pigment deposition in tobacco and in the unpigmented corolla limb region of *Nicotiana sylvestris*. Transcription studies showed that the organ, region, and cell specificities of the petal-specific genes are controlled primarily at the transcriptional level. We conclude that multitiered transcriptional regulatory processes act on genes during petal development to program their individual expression patterns.

RESULTS

A Pink Limb and a White Tube Form during Tobacco Corolla Development

Previously, we divided tobacco flower development into 19 stages (−7 to +12) to provide reference points for gene expression events during the differentiation of floral organ systems (Koltunow et al., 1990). Stage 1 was set as the period when anthers contain tetrads of microspores and stage 12 as the period of flower opening and pollen release. We designated stages −7 to −1 to describe events from floral primordia emergence to the completion of meiosis within the anthers. Stages 1 to 12 are shown in Figure 1A, and key markers for petal and corolla development are summarized in Table 1.

Figure 1A shows that the corolla of an open tobacco flower (stage 12) contains five fused petals and has a distinctive morphology and coloration pattern. The limb (L) at the top of the corolla contains horizontally expanded petal tips and is deep pink in color. By contrast, the vertically elongated tube (T) surrounds the pistil and stamens and is cream white. The top one-third of the tube bulges outward like a cup and contains a sharp pink/white boundary that marks the partition between the corolla limb and tube regions. Thus, there is a direct correlation between the morphological division of the corolla into the limb and tube, and the asymmetric distribution of pigmentation to form the pink/white coloration pattern.

Figure 1A shows that a pale green corolla emerges from the flower bud at stage 2 and that the tube expands vertically in length until stage 12, when horizontal limb extension and flower opening occur. Tube expansion occurs simultaneously with both style and filament elongation (Koltunow et al., 1990). In

Table 1. Markers for Tobacco Petal Development

Stage[a]	Bud Length[b]	Morphological Markers[c]
−8	≤0.50	Petal primordia emerge in second whorl; primordia between and below tips of stamen primordia.
−7	0.75	Five tooth-shaped petal primordia formed; midvein procambium differentiation begun; mitotic activity at margins; ground parenchyma and epidermal layers present.
−6	1.5	Petal fusion begins; lateral margin growth occurs; trichomes differentiating on abaxial surface.
−5	3	Petals fused at their margins; midvein vascular bundle differentiated; trichomes begin to appear; procambium differentiation occurring in margins.
−4	4	Corolla encloses anthers; petal tips at top of stamen primordia; many trichomes present on abaxial epidermal surface; vascular bundles scattered through the petal.
−1	7	Petal tips at top of sepals.
2	11	Pale green corolla emerges from darker green calyx.
3	14	Corolla above sepal tips; mesophyll green; limb epidermal cells brick-shaped and unpigmented; tube bulge formed.
5	20	Corolla tube bulge just inside calyx; limb epidermal surfaces flat and unpigmented; mesophyll green.
6	22	Corolla tube bulge at tip of calyx; corolla pale green.
7	28	Corolla tube bulge above calyx; petal tips closed; anthocyanin beginning to accumulate in petal tip epidermal cells; adaxial limb epidermal cell surface convex or papillate.
8	39	Corolla elongating rapidly; petals pale green; petal tips slightly open.
9	43	Corolla tube bulge enlarging horizontally and cup-shaped; petal tips visibly pink; anthocyanin in petal tip epidermal cells, papillae present on both limb epidermal layers; adaxial limb epidermal cells have nipple-like shape; mesophyll green.
10	45	Corolla limb begins to open; petal tips pink and expanding; tube becoming white.
11	47	Corolla limb halfway open; petal tips pink and expanding horizontally; limb epidermal cells deep pink; limb mesophyll layer green; limb adaxial epidermal papillae more dense and nipple-like than abaxial epidermal papillae; tube white.
12	46	Flower open; corolla limb fully expanded and deep pink; tube white in appearance; sharp pink/white border at top of tube cup-bulge.

[a] Stages described by Koltunow et al. (1990), except that stage −8 was added as the stage of petal and stamen primordia emergence. Sepal primordia already fully emerged and green at this stage.

[b] Taken from the data of Koltunow et al. (1990). Expressed in millimeters.

[c] Taken from Koltunow et al. (1990) and from the data presented in Figures 1A and 1B, and 2.

addition, expansion occurs from the base upward and increases rapidly between stages 7 and 8 (Table 1). At stage 6 the cup-bulge can be seen at the top of the corolla tube, and by stage 9 the petal tips within the developing limb are light pink, indicating that anthocyanin accumulation in this region has begun. Between stages 9 and 12, limb maturation, petal tip bending, and horizontal extension occur and the entire limb becomes deep pink in color. By contrast, the tube loses its greenish tinge during this period, and by stage 12 the characteristic pink/white tobacco corolla coloration pattern has formed. These observations indicate that there is a tight coupling between the period of limb maturation and the generation of the pink/white color pattern late in corolla development (Figure 1A and Table 1).

We made freehand sections of petal tips throughout corolla development to visualize cell differentiation and pigment accumulation events within the limb region. Figure 1B shows that at stages 3 and 5 the petal tips have unpigmented epidermal cell layers with flat, brick-like surfaces and a green mesophyll, which is responsible for generating the pale green corolla color at these developmental stages. In addition, trichomes are present on the abaxial epidermis (AbE). By contrast, both the adaxial epidermal (AdE) and abaxial epidermal layers contain anthocyanin pigments at stage 7, and large numbers of papillae, or convex bumps, have differentiated on the surface of the adaxial epidermis. Anthocyanin accumulation within the epidermal cells accelerates between stages 7 to 11 and is paralleled by the differentiation of papillae on the abaxial epidermis and conversion of the dense adaxial epidermal bumps into pointed, or nipple-like, structures (Figure 1B). These results indicate that there is a temporally regulated and cell-specific accumulation of anthocyanins within limb epidermal cells and that pink pigment accumulation is correlated with the differentiation of papillae on the epidermal surfaces.

We characterized early petal development (stages −7 to −1) to determine when major cell differentiation events occurred and when petals fused within the corolla. The scanning electron micrographs shown in Figure 2A indicate that the five petal primordia (P) emerged prior to stage −7 and by stage −5 elongated vertically to the tops of the differentiating stamen primordia (A). The bright-field sections shown in Figure 2B indicate that stage −7 petal primordia consist of adaxial (AdE) and abaxial (AbE) epidermal layers, lateral margins (LM), a central procambium region (V), and ground parenchyma (G). Figure 2B also shows that at stage −5 procambium differentiation into the midvein is complete, trichomes have differentiated on the abaxial epidermal surface, and that the petal primordia margins have expanded laterally and fused (FZ). Figures 2A and 2C show that by stage −4 fusion of adjacent petals is complete (FZ), numerous vascular bundles have formed, and the partitioning of the corolla into limb and tube regions has begun. Together, these data show that petal cell differentiation and fusion events take place early in flower development, and that most of the time from petal primordia emergence to flower opening involves establishment of the corolla tube and limb regions, tube elongation, limb maturation, and generation of the pink/white coloration pattern.

Tobacco Corolla Coloration Pattern and Morphology Are Inherited from *N. tomentosiformis*

We compared corolla development in *N. sylvestris* and *N. tomentosiformis*, the diploid progenitors of tobacco (Goodspeed, 1954; Gray et al., 1974; Okamuro and Goldberg, 1985), with that of tobacco. Figure 1C shows 12 stages of *N. sylvestris* flower development analogous to stages 1 to 12 for tobacco (Figure 1A). At flower opening (stage 12), the *N. sylvestris* corolla is approximately twice as long as the tobacco corolla (10 vs 4.5 cm) and is chalk white with no detectable pigmentation. The thin tube does not contain a cup-like bulge and the mature limb contains five star-shaped petal tips. Analogous to tobacco corolla development, *N. sylvestris* limb maturation and expansion occur between stages 9 to 12.

In contrast with these observations, Figure 1D shows that *N. tomentosiformis* has a corolla that closely resembles that of tobacco (Figure 1A). The *N. tomentosiformis* corolla is approximately one-half the size of the tobacco corolla (2.5 vs 4.5 cm), but has a similar coloration pattern—a pink limb and a greenish tube. In addition, the tube has a prominent green cup-bulge which occupies almost half the tube length. The cup-bulge forms early in corolla development (stages 1 to 2) and contains the pink/green coloration boundary (Figure 1D). *N. tomentosiformis* limb expansion and maturation occur during stages 9 to 12, and these events are coupled with the limb-specific accumulation of anthocyanins and the establishment of the pink/green coloration pattern analogous to the situation for tobacco (Figure 1A). Together, these observations suggest that the pink/white coloration pattern and shape of the tobacco corolla are inherited from *N. tomentosiformis*. We infer that genes controlling *N. tomentosiformis* corolla pigmentation pattern and shape are dominant to those specifying these characteristics in *N. sylvestris*.

Two Petal mRNA Classes Were Identified in Tobacco Limb and Tube cDNA Libraries

We constructed cDNA libraries for stage 12 corolla limb and tube regions (Figure 1A) and then screened these libraries for cDNA clones that (1) represented mRNAs present exclusively, or at elevated levels, in the petal and (2) were specific for each corolla region (see Methods). In addition, we isolated a tobacco chalcone synthase genomic clone (see Methods) because this gene encodes an enzyme in the anthocyanin pathway (Reimold et al., 1983; Koes et al., 1990; Jackson et al., 1992). We obtained 28 petal cDNA clones from screens of 768 plasmids from each library. Of these, 17 cDNA clones represented mRNAs present at a higher level in the limb compared with the tube, whereas 11 cDNA clones represented mRNAs present equally in both regions. No cDNA clones were identified that represented tube-specific mRNAs.

We sorted the 28 petal cDNA clones into 19 different sequence groups by a combination of restriction mapping, cross-hybridization, and RNA gel blot studies. The limb-specific cDNA clones were divided into nine different groups, whereas

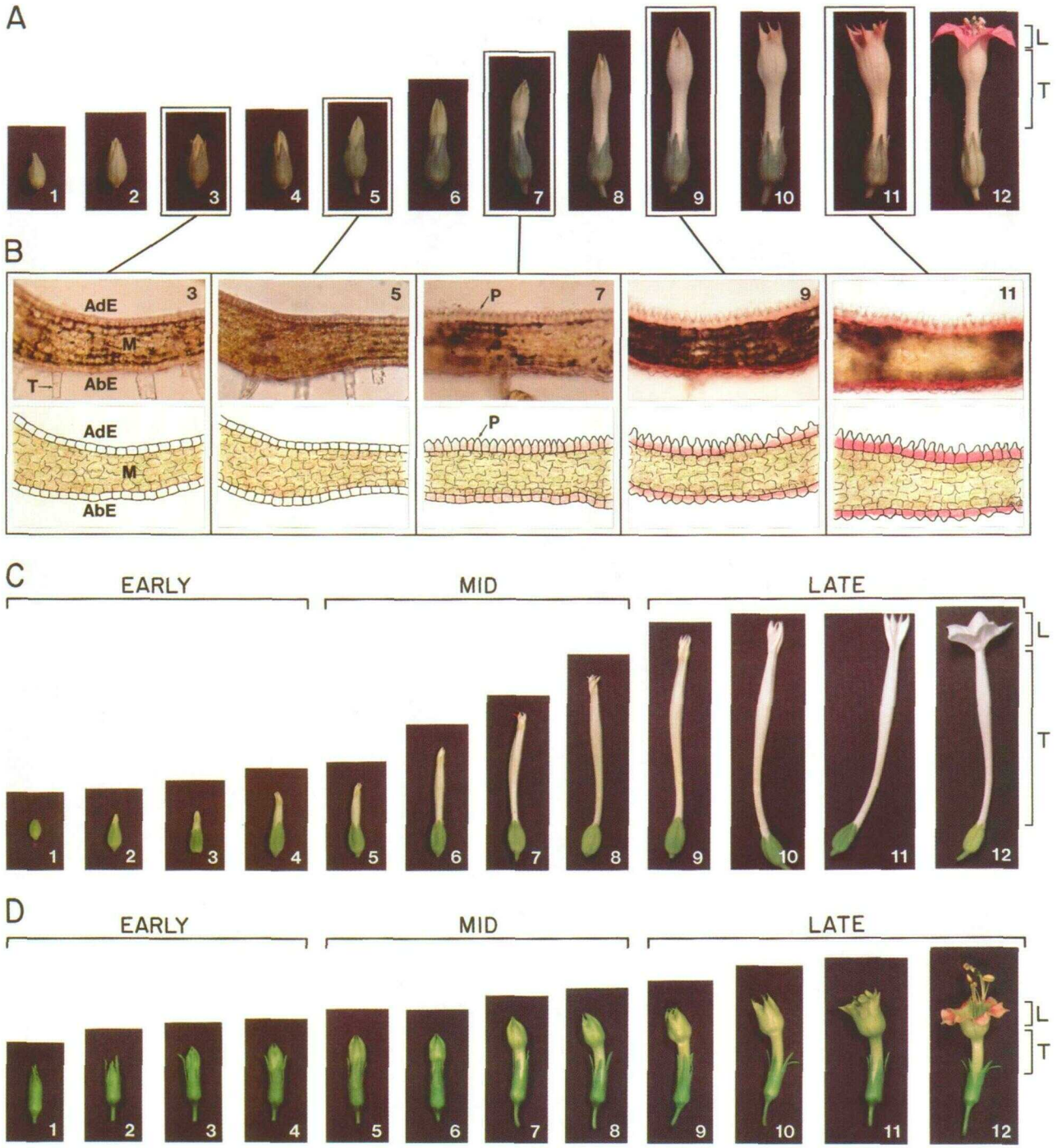

Figure 1. Petal Development in Tobacco and Progenitor Species.

those representing mRNAs present equally in the limb and the tube were sorted into 10 different groups. Table 2 lists representative cDNA clones from both classes as well as the chalcone synthase (CHS) genomic clone. DNA sequencing studies indicated that the limb-specific cDNA clones TP7 and TP12 represented isoflavone reductase mRNA (Paiva et al., 1991) and patatin mRNA (Bevan et al., 1986), respectively. Two other limb-specific cDNA clones sequenced (TP28 and TP29) failed to show relatedness to any known mRNA or protein.

We hybridized representative petal cDNA plasmids and a plasmid containing chalcone synthase coding sequences (see Methods) with gel blots containing stage 12 limb and tube mRNAs. Figure 3A shows that all of the probes produced strong hybridization signals with limb mRNA (L). We estimated that the prevalence of these mRNAs varied from 0.2% (CHS, TP13, TP28, TP29) to 3% (TP7) of the limb mRNA (Table 2). Each plasmid also hybridized with tube mRNA (T), as shown in Figure 3A. The ratio of limb to tube mRNA signals, however, varied with each probe (Table 2). For example, the TP12 patatin mRNA was 125 times more prevalent in the limb as compared to the tube, while the TP13, TP20, and TP29 mRNAs were only five times more prevalent in the limb than the tube. By contrast, the TP22 mRNA was present equally, or at a slightly higher level, in the tube as compared with the limb region (Table 2). Together, these data indicate that we have identified petal cDNA clones representing mRNAs that are either more prevalent in the limb than the tube or that are distributed equally in both corolla regions.

Petal mRNAs Are Present in Other Organ Systems

We hybridized representative petal plasmid DNA probes with gel blots containing leaf, stem, root, pistil, and anther mRNAs to determine the representation of petal mRNAs in other organs. The results, shown in Figure 3B and summarized in Table 3, indicated that each limb-specific probe (CHS, TP7, TP12, TP13, TP20, TP28, TP29) reacted with the mRNAs from one or more heterologous organs and had a distinctive hybridization pattern. Similar results were obtained with probes representing mRNAs present equally in the limb and tube corolla regions (TP22; Figure 3B and data not shown).

Table 3 indicates that the TP7 isoflavone reductase and TP29 mRNAs were represented in all heterologous organ mRNAs, but at levels 25- to 1000-fold lower than those found in whole petal mRNA, and at even lower levels relative to limb mRNA alone (Table 2). TP13 and TP20 mRNAs were also present in all heterologous vegetative and floral organ mRNAs, and in some cases (e.g., stem) their prevalences in other organs slightly exceeded those found in the petal (Figure 3B and Table 3). Relative to limb mRNA, however, the TP13 and TP20 mRNAs were present at lower concentrations in all heterologous organs (Tables 2 and 3). By contrast, the TP28 mRNA was detected only in the root, whereas the TP12 patatin mRNA was detected in root, pistil, and anther (Table 3). In each organ system, these mRNAs had lower prevalences than in the petal. These data indicate that most of the mRNAs investigated are present at higher levels in the petal relative to other organs and that a few are represented equally in one or more heterologous organs. Taken together with the results presented in Figure 3A and Table 2, these data indicate that no prevalent mRNAs were found that are present exclusively in either corolla region or in the petal as a whole.

Petal Gene Expression Is Temporally Regulated

We hybridized several limb-specific petal plasmid DNA probes (CHS, TP7, TP12, TP28, TP29) with mRNA from different stages of corolla development to determine whether their corresponding genes were regulated temporally. Figure 4A shows that all of the petal mRNAs were temporally regulated, and that each mRNA had a unique accumulation pattern throughout corolla development and during the period of limb maturation and anthocyanin deposition (stages 7 to 12, Figure 1A). For example, chalcone synthase mRNA accumulated early in corolla development (stages 1 to 3), remained relatively constant until just prior to the completion of limb maturation (stage

Figure 1. Petal Development in Tobacco and Progenitor Species.

(A) Tobacco petal development. Morphological events and key markers for petal development are outlined in Table 1. Stage 1 bud and stage 12 open flower sizes averaged 8 and 46 mm in length, respectively (Koltunow et al., 1990). L and T refer to the corolla limb and tube, respectively.
(B) Bright-field photographs of tobacco petal sections at different developmental stages. Freehand (unfixed) transverse sections were taken near petal tips within the limb region at stages 3, 5, 7, 9, and 11. AbE, AdE, M, P, and T refer to abaxial epidermis, adaxial epidermis, mesophyll, papillae, and trichome, respectively. Drawings below the photographs are schematic representations of petal anatomy and anthocyanin accumulation at each stage. Pink and green coloration represents anthocyanin and chlorophyll pigmentation, respectively.
(C) *N. sylvestris* petal development. *N. sylvestris* flower development was divided into 12 stages analogous to those of tobacco **(A)**. Stage 1 bud and stage 12 open flower sizes averaged 9 and 103 mm, respectively. The transition from stage 1 to stage 12 occurred over a 10-day period during the summer. L and T refer to the corolla limb and tube, respectively.
(D) *N. tomentosiformis* petal development. *N. tomentosiformis* flower development was divided into 12 stages analogous to those of tobacco **(A)**. Stage 1 bud and stage 12 open flower sizes averaged 7 and 25 mm, respectively. L and T refer to the corolla limb and tube, respectively. The time period for the stage 1 to stage 12 transition was not measured.

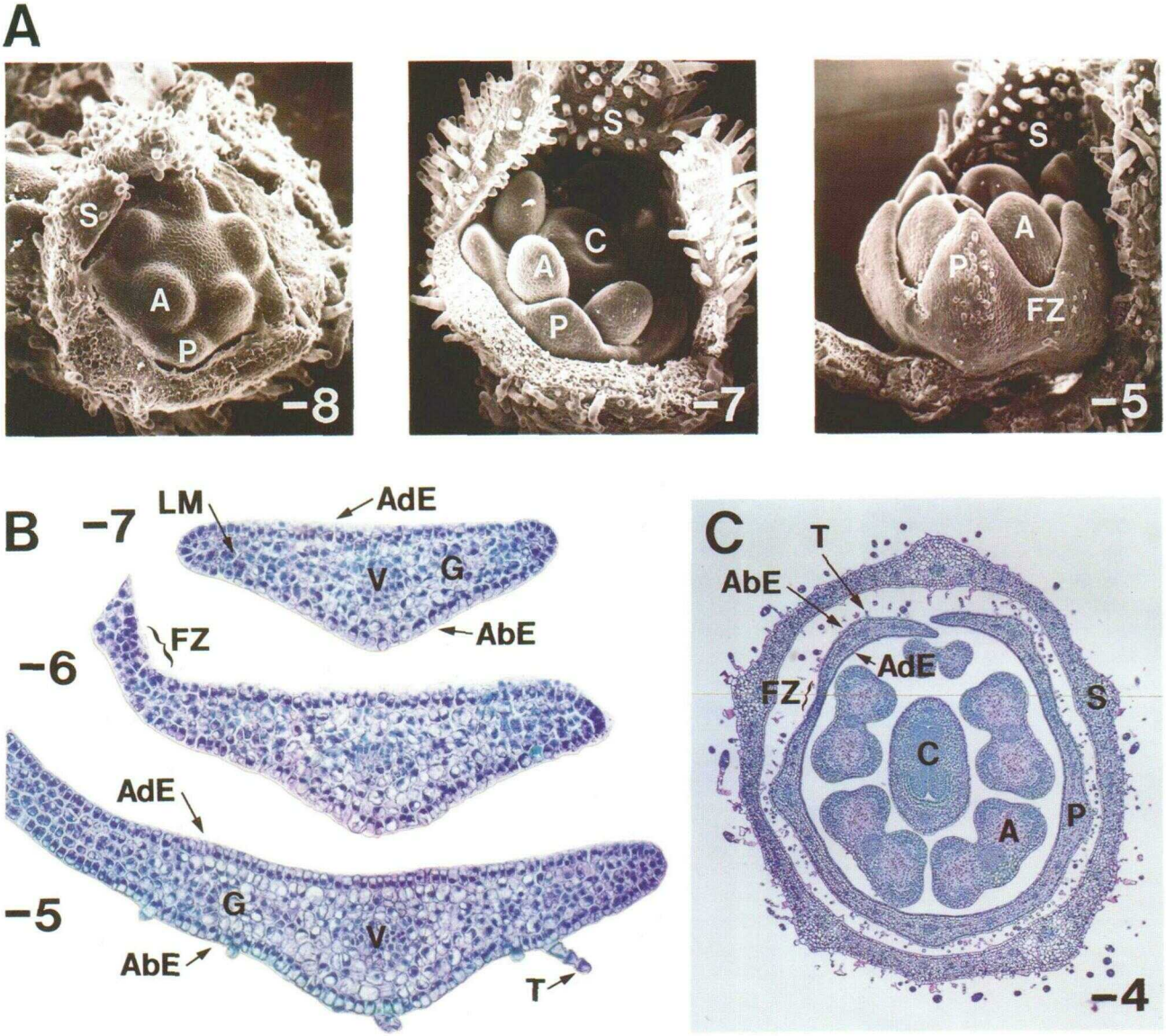

Figure 2. Early Tobacco Petal Development.

(A) Scanning electron micrographs of petal primordia during the early stages of flower development. Flower buds at the designated stages were harvested, sepals were removed to expose petal primordia, and then photographed in the scanning electron microscope, as outlined in Methods. A, C, FZ, P, and S refer to stamen, carpel, fusion zone, petal, and sepal, respectively.

(B) Bright-field photographs of petal sections early in development. Flower buds at the designated stages were harvested, fixed, embedded with paraffin, and sliced into 10-μm transverse sections, as described in Methods. The fixed sections were stained with toluidine blue and photographed with bright-field illumination. AbE, AdE, FZ, G, LM, T, and V refer to abaxial epidermis, adaxial epidermis, fusion zone, ground parenchyma, lateral margin, trichome, and vascular bundle, respectively.

(C) Bright-field photograph of an early floral bud section. Stage −4 flower buds were harvested, fixed, embedded, and sliced into 10-μm sections, as indicated in **(B)**. The toluidine blue sections were photographed with bright-field illumination. The noncontiguous portion of the corolla is due to the section angle, which is above the fusion zone in this area. A, C, FZ, P, and S refer to anther, carpel, fusion zone, petal (corolla), and sepal (calyx), respectively.

11), and then declined at flower opening (stage 12). By contrast, the TP28 mRNA was present at a low level throughout corolla development (stages 1 to 11) and then accumulated significantly at flower opening (stage 12). The TP7 isoflavone reductase, TP12 patatin, and TP29 mRNAs were also present at low levels early in corolla development (stages 1 to 7), but accumulated noncoordinately during later stages (stages 7 to 12). Together, these data show that several different

temporal patterns of mRNA accumulation occur during corolla development.

Region-Specific mRNA Accumulation Occurs Early in Corolla Development

Figure 4B shows a close-up of a stage 3 flower bud with its calyx (S) and corolla (C). As shown in Figure 4C, we divided the corolla of these buds into top (T), middle (M), and bottom (B) regions. We then hybridized the chalcone synthase probe with mRNAs isolated from each of these regions to determine whether this mRNA was localized regionally within the corolla early in development. The RNA gel blot shown in Figure 4D indicates that the chalcone synthase probe reacted more strongly with top- and middle-section mRNAs than with mRNA from the bottom section. These data indicate that at least one limb-specific mRNA is localized preferentially within the upper region of the corolla early in development, suggesting that at stage 3 the corolla is already divided into regions destined to become the limb and tube at maturation.

Petal mRNAs Are Localized in Different Cell Types

We utilized in situ hybridization with labeled single-stranded anti-mRNA probes to localize petal mRNAs within specific cell types (see Methods). Figure 5A shows a bright-field photograph of a petal tip section from the limb of stage 12 corollas. The adaxial (AdE) and abaxial (AbE) epidermal layers can be visualized in this section along with the mesophyll (M) and the central midvein (V). As seen in Figures 5B to 5F, two different mRNA localization patterns were observed within the petal. The TP7 isoflavone reductase, chalcone synthase, TP28, and TP29 mRNAs were all localized within the epidermal cells (Figures 5B to 5E). No hybridization grains above background levels were observed within the mesophyll or the vascular bundles. By contrast, the TP12 patatin mRNA was localized within parenchyma cells of the mesophyll (Figure 5F). No hybridization signals above background were observed within the vascular bundles or within the epidermal layers.

We hybridized the TP7 isoflavone reductase and TP12 patatin mRNA probes in situ with petal tip sections from different development stages to determine whether the epidermal-specific and mesophyll-specific patterns were the same throughout corolla development. Figure 6A shows a freehand section of a stage 9 petal tip with pink adaxial (AdE) and abaxial (AbE) epidermal layers and a green mesophyll (M). Figures 6B to 6E show that the TP7 isoflavone reductase mRNA accumulated simultaneously within both epidermal cell layers between stages 9 to 11 and that signals were not detected in other petal cell types during the period investigated (stages 9 to 12). Similarly, Figures 6F to 6J show that the TP12 patatin mRNA accumulated simultaneously within the mesophyll cells be-

Table 2. Characteristics of Tobacco Petal mRNAs

mRNA	Size[a]	Prevalence[b]	L/T Ratio[c]	Cell Specificity[d]	Protein Encoded[e]
CHS	1.5	0.2	10	Epidermis	Chalcone synthase[f]
TP7	1.2	3.0	40	Epidermis	Isoflavone reductase[g]
TP12	1.7	1.2	125	Mesophyll	Patatin[h]
TP13	1.0	0.2	5	ND[i]	ND[i]
TP20	1.1	0.2	5	ND[i]	ND[i]
TP28	1.6	0.2	10	Epidermis	Unknown
TP29	1.0,1.1	0.2	5	Epidermis	Unknown
TP22	1.6	ND[i]	0.5	ND[i]	ND[i]

[a] Taken from Figure 3.

[b] Percentage of stage 12 limb polysomal poly(A) mRNA. Estimated relative to calibrated RNA standards.

[c] mRNA prevalence ratio between the limb (L) and tube (T) regions of stage 12 corollas. Estimated by densitometric analysis of the RNA gel blots shown in Figure 3A.

[d] Cell localization within the limb region. Taken from the in situ hybridization data shown in Figures 5 to 7.

[e] Highest identity score with proteins in the GenBank. Unknown indicates that no related genes or proteins were found in the GenBank.

[f] Fifty-two percent identical and 92% similar at the amino acid level to the parsley pLF15 chalcone synthase (Reimold et al., 1983). Recently, we determined that the tobacco anther-specific TA46 mRNA (Koltunow et al., 1990) also encodes chalcone synthase and is 20% identical and 59% similar at the amino acid level to the CS2 chalcone synthase studied here (J. Seurinck, T. P. Beals, and R. B. Goldberg, unpublished results). In contrast to the CS2 chalcone synthase, which is petal-limb specific (Figure 3A) and is present at high levels in most anther cell types during the mid to late stages of anther development (Figure 9C; G. N. Drews and R. B. Goldberg, unpublished results), the TA46 chalcone synthase mRNA accumulates early in anther development (stages 1 to 3), is probably tapetal specific, and is not present at a high level in the petal (Koltunow et al., 1990).

[g] Fifty-six percent identical and 88% similar at the amino acid level to the alfalfa isoflavone reductase (Paiva et al., 1991).

[h] Fifty-two percent identical and 92% similar at the amino acid level to the potato class I patatin (Bevan et al., 1986).

[i] Experiment not carried out, or DNA sequence not determined.

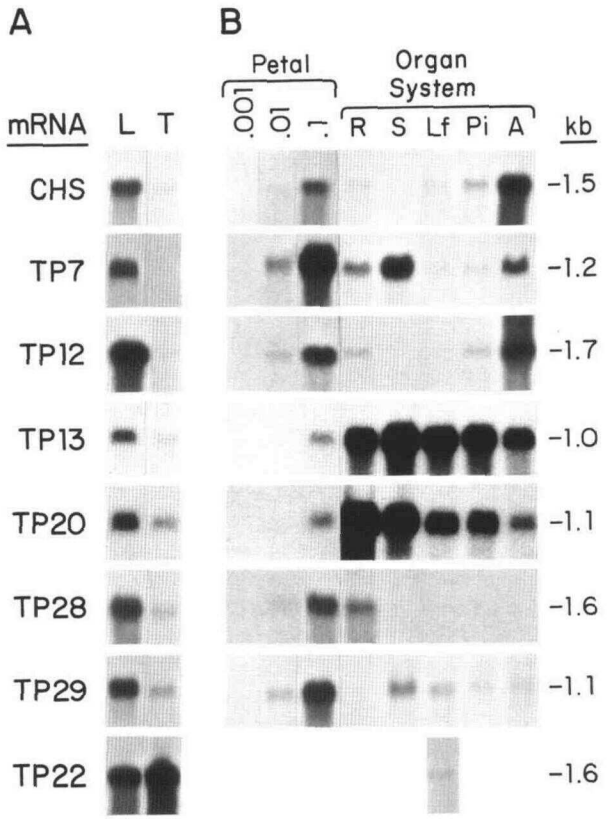

Figure 3. Representation of Petal mRNAs within the Corolla and Other Organ Systems.

Polysomal poly(A) mRNAs were isolated, fractionated by electrophoresis on denaturing agarose gels, transferred to nytran, and hybridized with each plasmid DNA probe, as outlined in Methods. Film exposure times varied for each gel blot, but were the same for all RNA lanes hybridized with a specific probe. CHS, chalcone synthase.

(A) Representation of petal mRNAs within the limb (L) and tube (T) of stage 12 corollas. Each RNA gel blot contained 0.5 μg of mRNA per lane.

(B) Representation of petal mRNAs in the root (R), stem (S), leaf (Lf), pistil (Pi), and anther (A). Each organ system gel blot lane contained 5 μg of mRNA, except for the anther lane of the CHS gel blot, which contained 0.5 μg of mRNA. The petal dilution lanes contained 0.5, 0.05, and 0.005 μg of stage 12 whole corolla (limb plus tube) mRNA representing prevalences of 10%, 1%, and 0.1% relative to petal mRNA, respectively. Only leaf mRNA was used for the TP22 gel blot. Stage 6 mRNAs were used for the pistil and anther gel blot lanes.

tween stages 6 to 10, and that no hybridization signals above background were observed over the epidermal cell layers or vascular tissues at any stage of development studied (stages 5 to 12). As predicted from the RNA dot blot studies (Figure 4A), the TP12 patatin mRNA accumulated slightly earlier than the TP7 isoflavone reductase mRNA (Figures 6B to 6J). Together, these data show that limb-specific mRNAs are localized in either the epidermis or the mesophyll, and that these cell localization patterns occur at different stages of corolla development.

Epidermal- and Mesophyll-Specific mRNAs Simultaneously Decline within the Limb/Tube Border Region

We hybridized limb-mesophyll–specific (TP12) and limb-epidermal–specific (CHS, TP7, TP28, TP29) anti-mRNA probes in situ with stage 12 corolla longitudinal sections to follow the decline in prevalence of these mRNAs at the cell level within the limb/tube transition zone (Figures 1A and 3A). Figure 7A shows a freehand section of the corolla limb/tube border, and Figure 7B shows a schematic representation of this section. As seen in Figures 7A and 7B, the transition from limb to tube occurs abruptly over a distance of approximately 15 epidermal cells and is marked by both pigmentation and morphological differences between these corolla regions. The limb adaxial (AdE) and abaxial (AbE) epidermal layers were pink due to anthocyanin accumulation and their surfaces contained papillae (Figures 1B, 7A, and 7B). By contrast, the tube epidermal layers were unpigmented and had flat surfaces (Figures 7A and 7B) analogous to those in the limb region prior to stage 7 (Figure 1B). The mesophyll layers in both regions were green (Figure 7A); however, tube mesophyll cells were packed more tightly together than those in the limb (data not shown).

Figure 7C shows that chalcone synthase mRNA decreased precipitously in prevalence within the epidermis of the limb/tube transition zone. In contrast to the results obtained with petal tip sections (Figure 5C), however, chalcone synthase mRNA was detected only in adaxial limb epidermal cells in the border region. Figure 7D shows that TP12 patatin mRNA declined

Table 3. Representation of Petal mRNAs in Heterologous Organs

	Percent Corolla mRNA[a]				
mRNA	Root[b]	Stem[b]	Leaf[b]	Pistil[c]	Anther[c]
CHS	0.5	<0.05[d]	0.8	1	200
TP7	1	4	0.1	0.1	1
TP12	2	<0.05[d]	<0.05[d]	1	40
TP13	100	170	90	150	40
TP20	190	110	50	50	20
TP28	5	<0.05[d]	<0.05[d]	<0.05[d]	<0.05[d]
TP29	0.2	2	1	0.9	1

[a] Polysomal poly(A) mRNA from stage 12 corollas (limb plus tube). Estimated by densitometric analysis of the RNA gel blot data shown in Figure 3B.

[b] Developmental characteristics described in Kamalay and Goldberg (1980).

[c] Taken from stage 6 flowers (Figure 1A).

[d] Below the detection level of the RNA gel blots shown in Figure 3B.

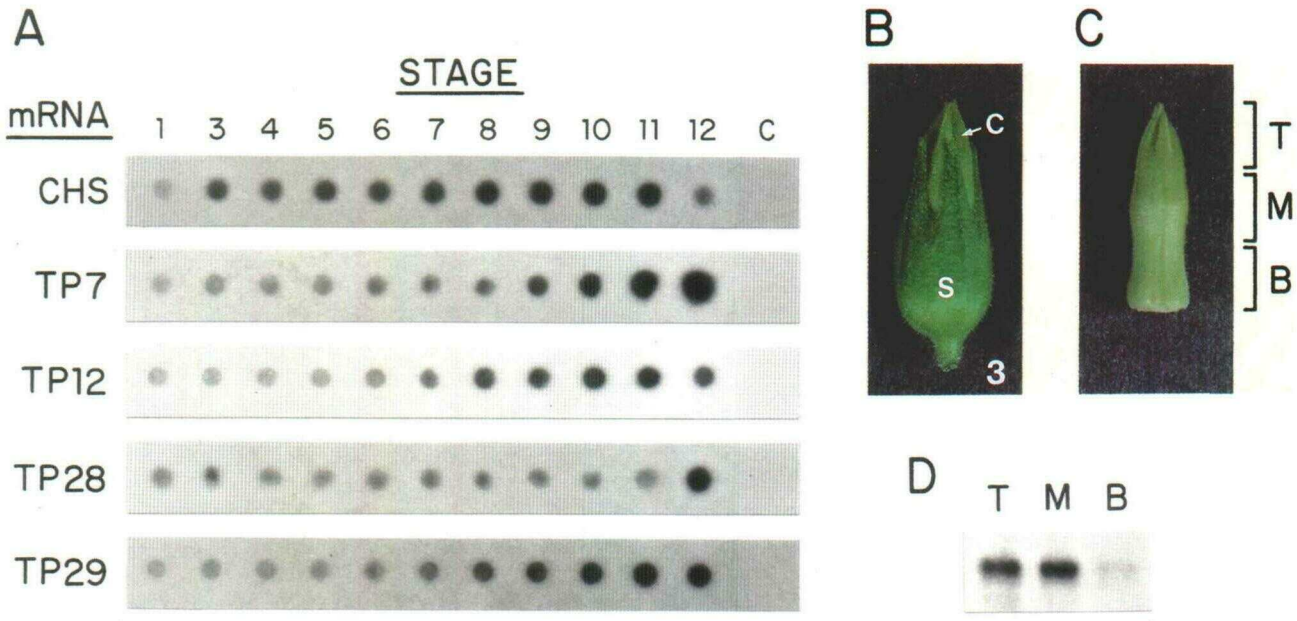

Figure 4. Accumulation of Petal mRNAs during Corolla Development.

(A) Temporal accumulation of petal mRNAs. Polysomal poly(A) mRNAs were isolated from whole corollas (limb plus tube) at different developmental stages (Figure 1A), spotted onto nytran filters, and hybridized with labeled plasmid DNA probes, as described in Methods. Dot blots contained between 0.05 and 0.2 μg of mRNA per dot, but all dots within a developmental series contained the same amount of mRNA. The control RNA dot (C) contained soybean embryo mRNA. Film exposure times varied for each developmental series with a given probe. Films were underexposed so that each mRNA accumulation pattern could be visualized accurately.

(B) Stage 3 flower bud. C and S refer to corolla and calyx, respectively.

(C) Regions of the corolla contained within a stage 3 flower bud **(B)**. T, M, and B refer to top, middle, and bottom, respectively. The top region contains the petal tips and the developing corolla limb region.

(D) Accumulation of chalcone synthase mRNA in different regions of a stage 3 corolla **(C)**. Polysomal poly(A) mRNA was isolated from the top (T), middle (M), and bottom (B) regions of stage 3 corollas, fractionated by electrophoresis on denaturing agarose gels, transferred to nytran, and hybridized with a labeled chalcone synthase probe, as described in Methods. Each lane contained 1.5 μg of mRNA.

in concentration within the mesophyll layer of the limb/tube border, and that this decrease occurred over the same 15-cell distance as the chalcone synthase mRNA (Figure 7C). Similar results were obtained for the TP7 isoflavone reductase, TP28, and TP29 epidermal-specific mRNAs (data not shown). Together, these results show that epidermal- and mesophyll-specific limb mRNAs decrease coordinately in prevalence within their respective cell types across the limb/tube border.

Petal mRNAs Are Localized in Specific Cell Types of Heterologous Organs

Figure 3B shows that the petal mRNAs investigated are represented in heterologous vegetative and floral organ systems. We carried out in situ hybridization experiments with both limb-epidermal–specific (TP7, CHS) and limb-mesophyll–specific (TP12) anti-mRNA probes to localize these sequences in heterologous organ cell types.

The TP7 Isoflavone Reductase mRNA Is Localized in Stem Xylem Cells

Figure 8 shows the localization pattern for the TP7 isoflavone reductase mRNA in the stem. We chose this organ because the TP7 isoflavone reductase mRNA had its highest prevalence in the stem relative to other heterologous organs (Figure 3B). Figure 8A shows a bright-field photograph of a vegetative stem transverse section containing epidermis (E), cortex (C), pith (P), xylem (X), inner phloem (IP), and external phloem (XP) tissues. As seen in Figure 8B, the TP7 isoflavone reductase anti-mRNA probe produced an intense hybridization signal over the xylem. Hybridization signals over other tissues and cell types, including the epidermis, were not detectably different from those obtained with the TP7 mRNA control probe shown in Figure 8C. Figure 8D is a magnification of the dark-field photograph shown in Figure 8B and shows that the TP7 isoflavone reductase mRNA is localized specifically within differentiating xylem cells and is not detectable within mature, differentiated

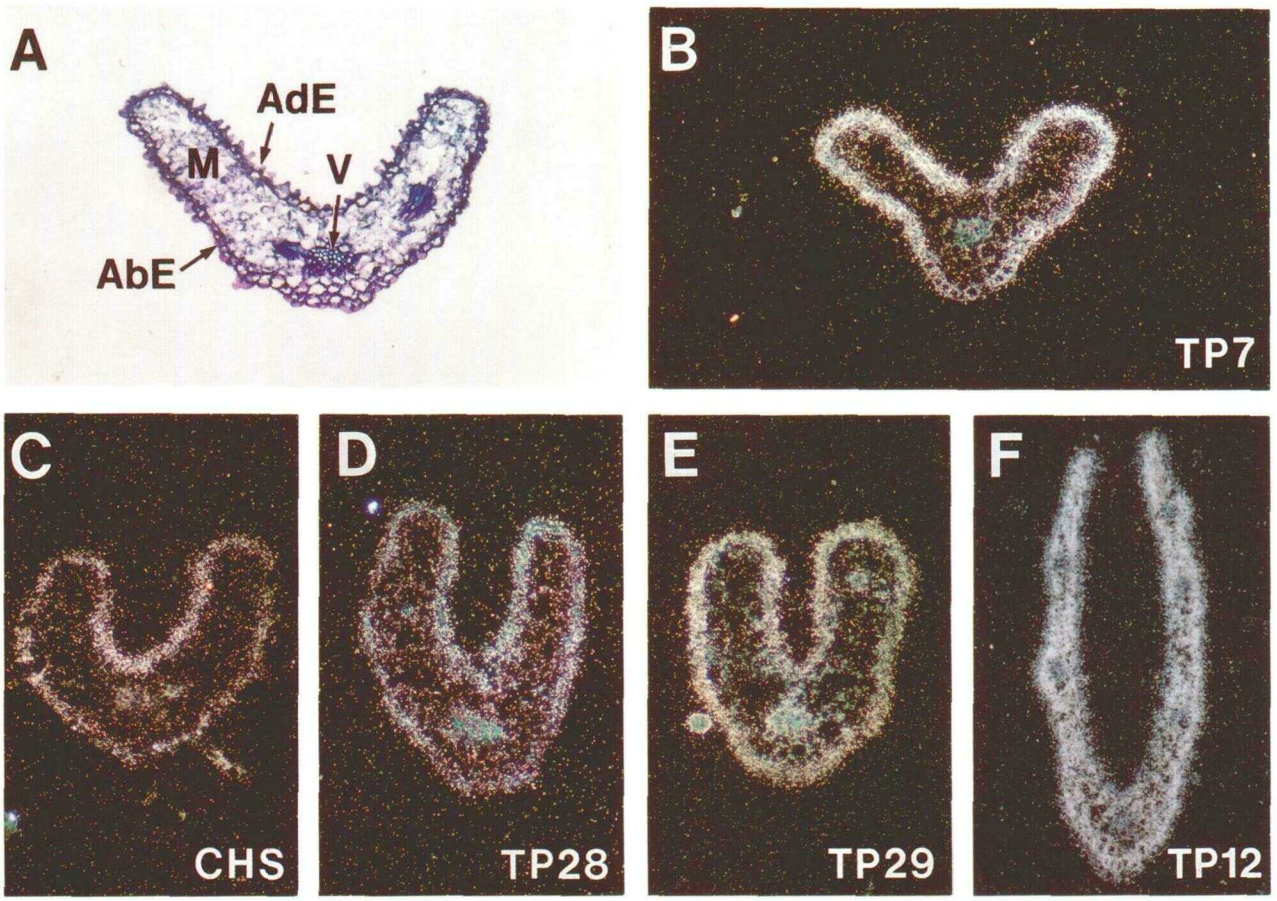

Figure 5. Localization of mRNAs within Petal Cell Types.

Petal tips from the limb region of stage 10 corollas (TP12) or stage 12 corollas (TP7, CHS, TP28, TP29) were fixed, embedded in paraffin, sliced into 10-μm transverse sections, and hybridized with single-stranded ^{35}S-RNA probes, as outlined in Methods.

(A) Bright-field photograph of a petal tip transverse section. AbE, AdE, M, and V refer to abaxial epidermis, adaxial epidermis, mesophyll, and vascular bundle, respectively.

(B) to **(F)** *In situ hybridization of petal tip transverse sections* with a TP7 anti-mRNA probe **[(B)]**, a chalcone synthase (CHS) anti-mRNA probe **[(C)]**, a TP28 anti-mRNA probe **[(D)]**, a TP29 anti-mRNA probe **[(E)]**, and a TP12 anti-mRNA probe **[(F)]**. White grains represent regions containing RNA/RNA hybrids. Photographs were taken by dark-field microscopy. Film emulsion exposure times varied for each probe.

xylem. A similar result was obtained with floral stem sections (Goldberg, 1988; R. Yadegari and R. B. Goldberg, unpublished results). Together, these data indicate that the TP7 isoflavone reductase mRNA, or a close relative, is localized within stem xylem cells and not in the epidermis as it is in the petal (Figures 5 and 6).

Chalcone Synthase and TP12 Patatin mRNAs Are Both Localized in the Anther Connective Region

Figure 3B shows that the chalcone synthase and TP12 patatin mRNAs had their highest prevalences in the anther relative to other heterologous organ systems. The localization pattern for these mRNAs in the anther is shown in Figure 9. A bright-field photograph of a stage 7 anther transverse section showing the epidermis (E), pollen sacs (PS), connective (C), vascular bundle (V), wall layers (W), and stomium (S) is presented in Figure 9A. As seen in Figure 9B, the TP12 patatin mRNA is localized primarily within the connective at this stage of anther development. No detectable hybridization grains above background levels were observed in other anther regions. By contrast, Figure 9C shows that the chalcone synthase mRNA is localized throughout the anther at stage 7, including the connective, wall layers, epidermis, and stomium regions. These data show that chalcone synthase and TP12 patatin mRNAs, or their close relatives, are present within at least one common cell type (connective parenchyma) in the anther, even though

these mRNAs are localized in different petal cell types (Figures 5C, 5F, 7C, and 7D). Taken together with the TP7 results shown in Figures 8B and 8D, these data indicate that the localization patterns of petal mRNAs differ between the corolla and heterologous organ systems.

Most Tobacco Petal Genes Are Represented in Both the *N. sylvestris* and *N. tomentosiformis* Genomes

We hybridized several petal plasmid DNA probes (CHS, TP7, TP12, TP28, TP29) with gel blots containing tobacco, *N. sylvestris*, and *N. tomentosiformis* DNAs to estimate the copy number of individual petal genes in the tobacco genome and to determine whether these genes were derived from one or both diploid parental species. Figure 10 shows that at the moderately stringent hybridization criterion employed (42°C, 50% formamide, 1 M Na^+), each probe reacted strongly with one to five single-copy DNA fragments and weakly with a small number (≤ 4) of other faint, or divergent, DNA fragments in the tobacco genome (lane T). For example, the CHS probe hybridized with five tobacco EcoRI DNA fragments at intensities equal to that of the single-copy DNA control (lane 1X) and hybridized weakly to two additional DNA fragments. By contrast, the TP29 probe hybridized with single-copy DNA intensity to only one tobacco EcoRI DNA fragment and reacted very faintly with

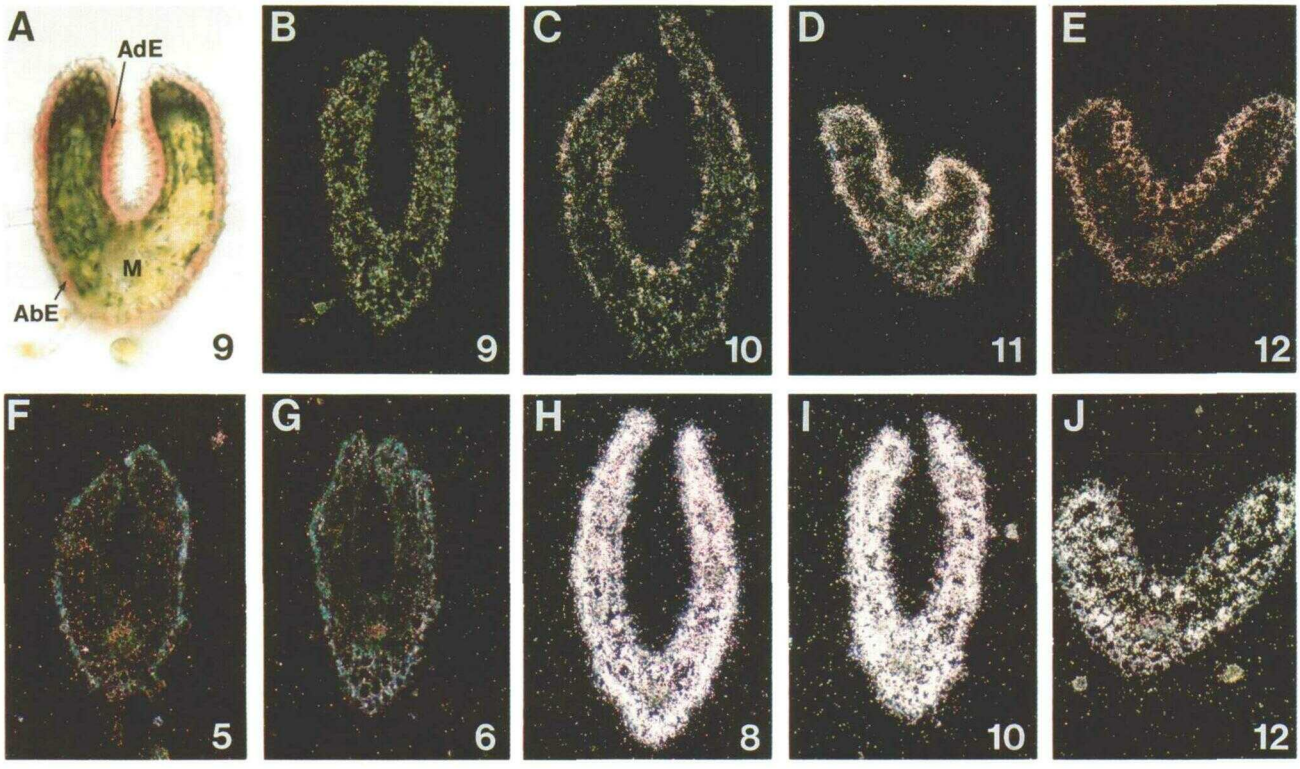

Figure 6. Temporal Accumulation of mRNAs in Petal Cell Types.

Petal tips from corollas at different stages of development were fixed, embedded in paraffin, sliced into 10-μm transverse sections, and hybridized with single-stranded ^{35}S-RNA probes, as outlined in Methods.

(A) Bright-field photograph of a freehand (unfixed) section through the petal tips in the limb region of a stage 9 corolla (Figure 1A). AdE, AbE, and M refer to adaxial epidermis, abaxial epidermis, and mesophyll, respectively. Pink and green coloration is due to anthocyanin and chlorophyll pigmentation, respectively.

(B) to **(E)** In situ hybridization of a TP7 anti-mRNA probe with petal tip transverse sections from corolla limb regions at stage 9 **[(B)]**, stage 10 **[(C)]**, stage 11 **[(D)]**, and stage 12 **[(E)]**. Photographs were taken by dark-field microscopy. White grains in the petals at stage 10 **[(C)]**, stage 11 **[(D)]**, and stage 12 **[(E)]** represent regions containing RNA/RNA hybrids. Film emulsion exposure times were the same for all stages.

(F) to **(J)** In situ hybridization of a TP12 anti-mRNA probe with petal tip transverse sections from corolla limb regions at stage 5 **[(F)]**, stage 6 **[(G)]**, stage 8 **[(H)]**, stage 10 **[(I)]**, and stage 12 **[(J)]**. Photographs were taken by dark-field microscopy. White grains in the petals at stage 8 **[(H)]**, stage 10 **[(I)]**, and stage 12 **[(J)]** represent regions of RNA/RNA hybrids. Film emulsion exposure times were the same for all stages.

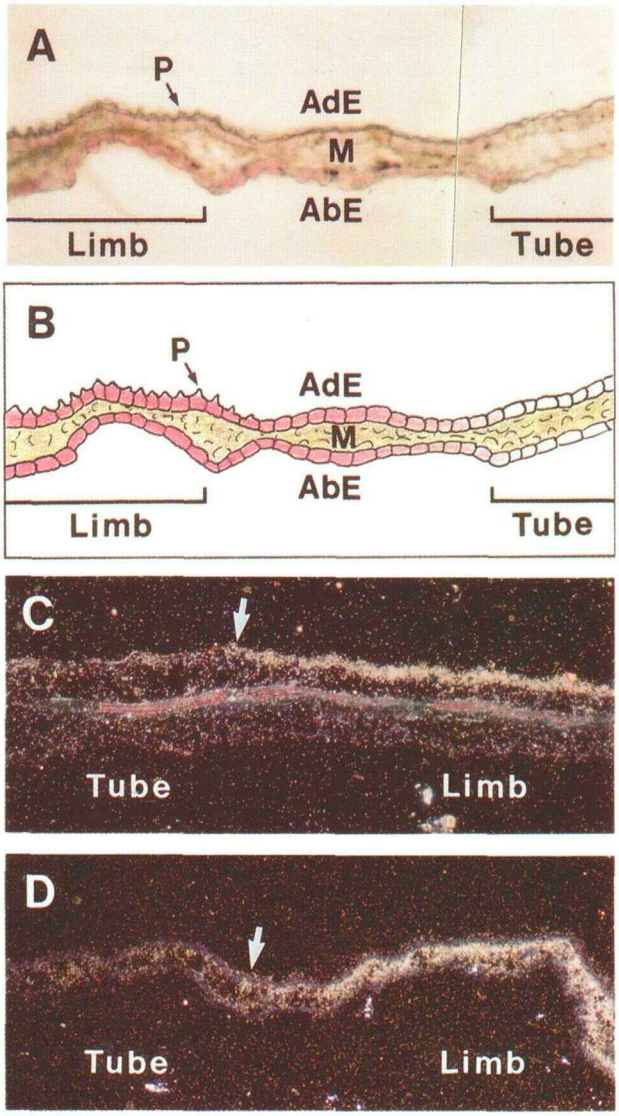

Figure 7. Localization of Petal mRNAs at the Corolla Limb/Tube Border.

Corollas from stage 12 open flowers (Figure 1A) were fixed, embedded in paraffin, sliced into 10-μm longitudinal sections at the limb/tube border, and hybridized with single-stranded ^{35}S-RNA probes, as outlined in Methods. AdE, AbE, M, and P refer to adaxial epidermis, abaxial epidermis, mesophyll, and papillae, respectively.

(A) Bright-field photograph of a stage 12 corolla freehand (unfixed) longitudinal section at the limb/tube border. Pink and green coloration is due to anthocyanin and chlorophyll pigments, respectively.

(B) Schematic representation of the bright-field photograph shown in **(A)**.

(C) In situ hybridization of a chalcone synthase anti-mRNA probe with a corolla longitudinal section at the limb/tube border. White grains in the limb region represent cells containing RNA/RNA hybrids. Arrow designates the limb/tube border. Photograph was taken by dark-field microscopy.

(D) In situ hybridization of a TP12 anti-mRNA probe with a corolla longitudinal section at the limb/tube border. White grains in the limb region represent cells containing RNA/RNA hybrids. Arrow designates the limb/tube border. Photograph was taken by dark-field microscopy. Film exposure time was the same as that shown in **(C)**.

four other divergent fragments. These results indicate that each petal gene studied is represented by a small number of highly homologous DNA sequences in the tobacco genome and that divergent relatives of these sequences also exist.

Figure 10 shows that four of the petal plasmid DNA probes (CHS, TP7, TP12, TP28) reacted strongly with one to three EcoRI DNA fragments in both the *N. sylvestris* (lane S) and *N. tomentosiformis* (lane To) genomes and weakly with a few (≤4) other DNA fragments in each genome, depending upon the probe. These fragments, however, were highly polymorphic and had different sizes in each genome, in agreement with the significant divergence that has taken place between *N. sylvestris* and *N. tomentosiformis* DNAs (Okamuro and Goldberg, 1985). By contrast, the TP29 probe hybridized strongly with one *N. tomentosiformis* EcoRI DNA fragment and only produced faint hybridization signals with *N. sylvestris* DNA (Figure 10). Close inspection of the DNA gel blots shown in Figure 10 indicates that, with the exception of some minor polymorphisms (lower case letters), the tobacco DNA gel blot pattern with each petal probe represents the union of patterns obtained with *N. sylvestris* and *N. tomentosiformis* DNAs. Taken together, these results indicate that most of the tobacco petal genes studied have highly related counterparts in both the *N. sylvestris* and *N. tomentosiformis* genomes, that the TP29 gene is probably derived from *N. tomentosiformis*, and that the petal genes have not diverged significantly since the time that *N. tomentosiformis* and *N. sylvestris* hybridized to form the allotetraploid tobacco genome.

Tobacco Petal mRNAs Are Regulated Regionally in *N. sylvestris* and *N. tomentosiformis* Corollas

We hybridized several tobacco limb-specific plasmid DNA probes (CHS, TP7, TP12, TP28, TP29) with *N. sylvestris* and *N. tomentosiformis* stage 12 limb and tube mRNAs (Figures 1C and 1D) to determine whether petal gene expression was also regulated regionally in the progenitor corollas. We were particularly interested in *N. sylvestris*, because this species has an unpigmented limb and tube (Figure 1C). The gel blots shown in Figure 11A indicate that the chalcone synthase, TP7 isoflavone reductase, TP12 patatin, and TP28 probes produced stronger signals with *N. sylvestris* limb mRNA (L) than with tube mRNA (T). As predicted from the DNA gel blots shown in Figure 10, the TP29 probe did not produce a detectable signal with either the *N. sylvestris* limb or tube mRNAs at film exposure times equivalent to those used for the other probes (Figure 11A, TP29 blank blot). Upon very long exposure, however (Figure 11A, TP29 asterisk blot), limb and tube mRNA

signals of approximately equal strength were observed with several, different-sized mRNAs, suggesting that divergent relatives of the TP29 gene were expressed in the *N. sylvestris* corolla.

Figure 11B shows that the chalcone synthase and TP7 isoflavone reductase probes produced stronger hybridization signals with *N. tomentosiformis* limb mRNA (L) than with tube mRNA (T). The TP29 probe also hybridized with *N. tomentosiformis* limb and tube mRNAs. However, in striking contrast to the results obtained with tobacco (Figure 3A and Table 2), the hybridization signal obtained with *N. tomentosiformis* tube mRNA was greater than that observed with mRNA from the limb (Figure 11B). Figure 11B also shows that the TP12 patatin and TP28 probes (asterisk blots) produced very weak, or undetectable, hybridization signals with *N. tomentosiformis* limb and tube mRNAs, suggesting that homologs of these genes were not expressed in the *N. tomentosiformis* corolla. Together, these results show that (1) tobacco petal gene homologs are expressed in the corolla of either *N. sylvestris* (TP12, TP28), *N. tomentosiformis* (TP29), or both progenitor species (CHS, TP7); (2) most of the petal genes retain their limb specificities

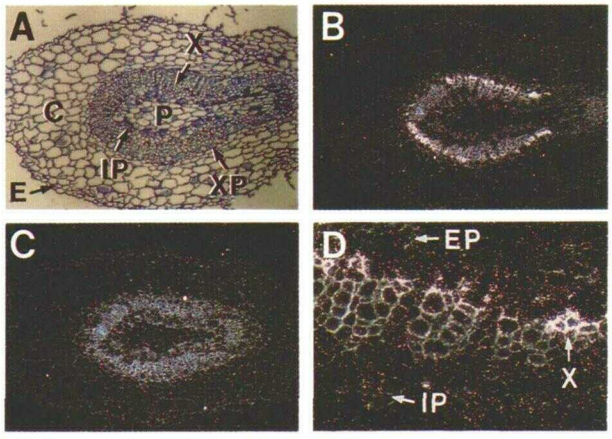

Figure 8. Localization of the TP7 Isoflavone Reductase mRNA within the Stem.

Stems were fixed, embedded in paraffin, sliced into 10-μm transverse sections, and hybridized with a TP7 anti-mRNA probe, as outlined in Methods. C, E, EP or XP, IP, P, and X refer to cortex, epidermis, external phloem, internal phloem, pith, and xylem, respectively.

(A) Bright-field photograph of a stem transverse section.

(B) In situ hybridization of a stem transverse section with a TP7 anti-mRNA probe. White grains within the xylem represent regions containing RNA/RNA hybrids. Photograph was taken with dark-field microscopy.

(C) In situ hybridization of a stem transverse section with a TP7 mRNA control probe. Photograph was taken with dark-field microscopy. White area in the vascular tissue region is due to light-scattering effects through the stained stem section.

(D) Dark-field photograph of the in situ hybridization experiment shown in **(B)** at five times higher magnification.

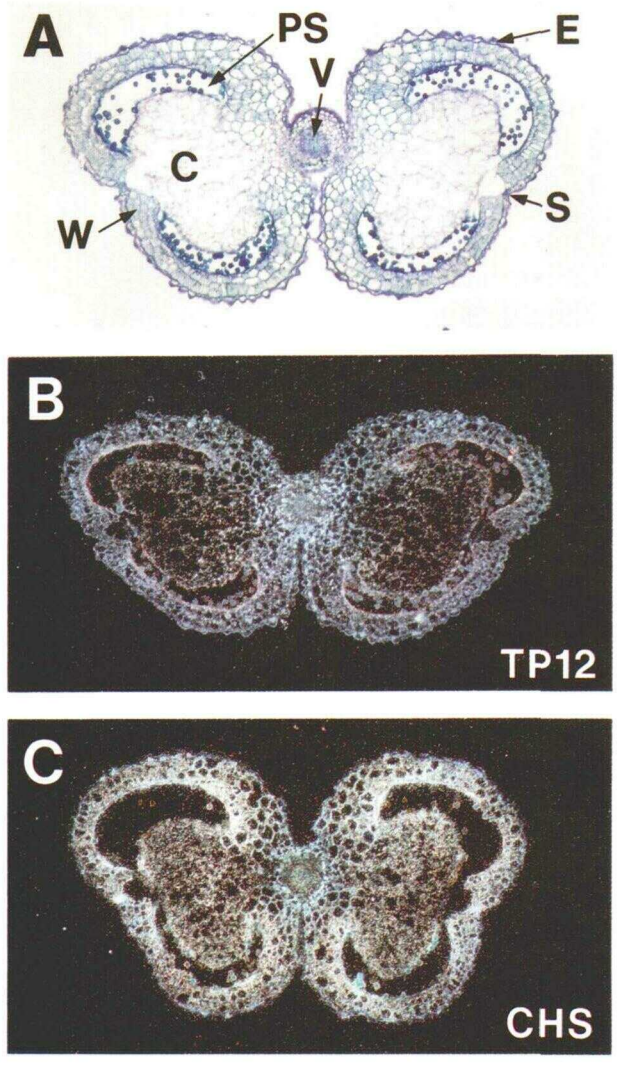

Figure 9. Localization of Chalcone Synthase and TP12 Patatin mRNAs within the Anther.

Anthers were fixed, embedded in paraffin, sliced into 10-μm sections, and hybridized with single-stranded ^{35}S-RNA probes, as outlined in Methods.

(A) Bright-field photograph of a stage 7 anther (Koltunow et al., 1990). C, E, PS, V, S, and W refer to connective, epidermis, pollen sac, vascular bundle, stomium, and wall layers, respectively.

(B) and **(C)** In situ hybridization of a TP12 patatin anti-mRNA probe **[(B)]** and a chalcone synthase anti-mRNA probe **[(C)]** with stage 7 anther sections. Photographs were taken by dark-field microscopy and white grains represent regions of RNA/RNA hybridization. White patchy areas in the walls of the TP12 anther **[(B)]** represent light-scattering effects due to dark-field illumination through the stained section. Film emulsion exposure times were the same for each probe.

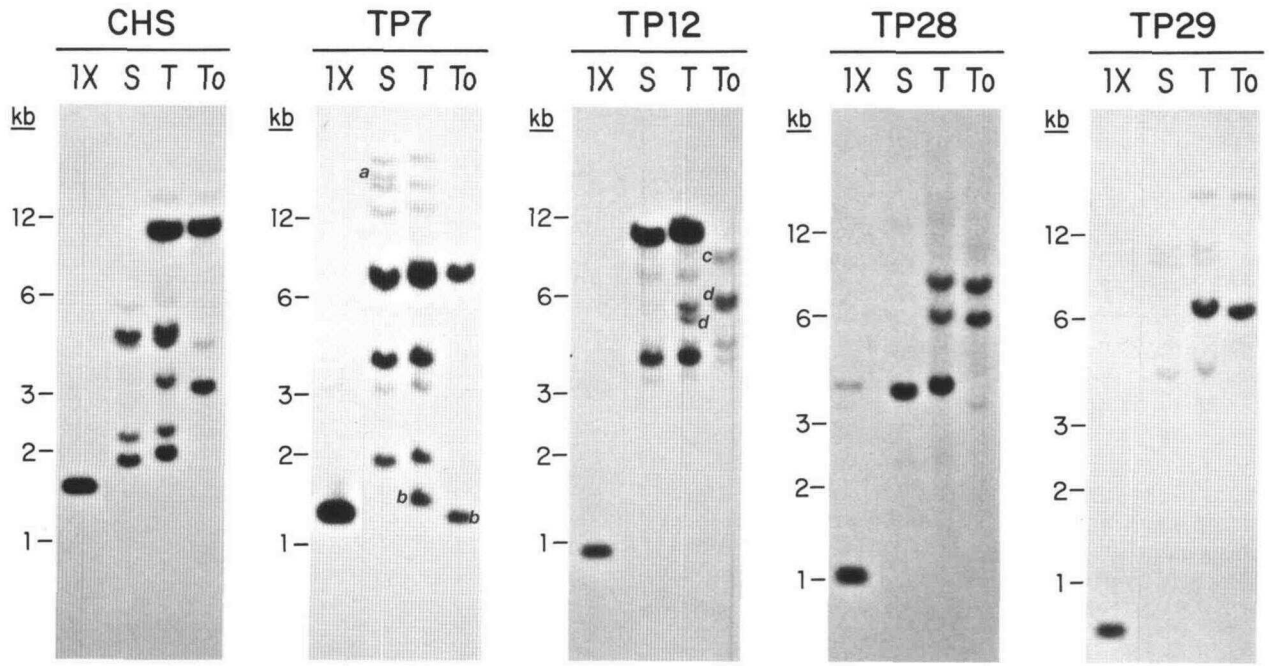

Figure 10. Representation of Petal mRNA Sequence in Tobacco Genomes.

Tobacco DNAs were digested with EcoRI, fractionated by electrophoresis on agarose gels, transferred to nytran, and hybridized with plasmid DNA probes, as outlined in Methods. The reconstruction lanes (1X) contained a single-copy equivalent of EcoRI-digested plasmid DNA and were calculated using a tobacco (*N. tabacum*) genome size of 2.4×10^6 kb (Okamuro and Goldberg, 1985). CHS, S, T, and To refer to chalcone synthase, *N. sylvestris*, tobacco (*N. tabacum*), and *N. tomentosiformis* DNAs, respectively. a, b, c, and d highlight restriction fragment length polymorphisms between the tobacco genome and those of the progenitor species.

irrespective of corolla coloration pattern; and (3) the TP29 gene is tube specific in *N. tomentosiformis* in contrast to its limb specificity in tobacco.

Tobacco Petal mRNAs Are Regulated Temporally during *N. sylvestris* and *N. tomentosiformis* Corolla Development

We hybridized several tobacco petal plasmid DNA probes (CHS, TP7, TP12, TP28, TP29) with gel blots containing mRNAs from different stages of *N. sylvestris* and *N. tomentosiformis* corolla development to determine whether the petal genes expressed in these plants were also regulated temporally. We utilized pools of early (stages 1 to 4), middle (stages 5 to 8), and late (stages 9 to 12) developing corollas for these experiments, as shown in Figures 1C and 1D. Figures 11A and 11B show that most of the petal mRNAs detected in *N. sylvestris* and *N. tomentosiformis* corollas were regulated temporally and that the mRNA accumulation patterns were similar to those observed during tobacco corolla development (Figure 4A). For example, the TP7 isoflavone reductase mRNA accumulated primarily during the middle (M) to late (Lt) periods of both *N. sylvestris* corolla development (Figure 11A) and *N. tomentosiformis* corolla development (Figure 11B), and the mRNA accumulation patterns for both TP7 homologs were similar to that observed in tobacco (Figure 4A). The TP28 mRNA accumulated only during the late (Lt) stages of *N. sylvestris* corolla development (Figure 11A), as was the case in tobacco (Figure 4A). By contrast, the chalcone synthase mRNA accumulation pattern differed in *N. sylvestris* and *N. tomentosiformis.* Chalcone synthase mRNA was present at relatively constant levels during the early (E), middle (M), and late (Lt) stages of *N. tomentosiformis* corolla development (Figure 11B), similar to the accumulation pattern in tobacco (Figure 4A). The *N. sylvestris* chalcone synthase homolog, however, gradually accumulated throughout *N. sylvestris* corolla development (Figure 11A). Together, these data indicate that the tobacco petal genes retained the temporal expression programs that originated in their diploid progenitors.

Petal Gene Expression Patterns Are Regulated at the Transcriptional Level

Region Specificity

We hybridized DNA gel blots containing limb-specific plasmid DNAs (CHS, TP7, TP12, TP28, TP29) with ^{32}P-nuclear RNAs synthesized in isolated stage 12 corolla limb and tube nuclei

to determine whether corolla-region–specific expression patterns were regulated at the transcriptional level. As a control, we included a plasmid DNA (TP22) that represents an mRNA present equally in limb and tube regions (Figure 3A and Table 2).

Figure 12A shows that all plasmid DNAs, except TP12, hybridized with limb ^{32}P-nuclear RNA at varying intensities. TP7 produced the strongest hybridization signal, consistent with its high prevalence in limb mRNA (Table 2). Absence of a TP12 signal suggests that the TP12 patatin gene is either inactive in the corolla at stage 12 or that it is transcribed below the detection level of our gel blots. Figure 12B shows that none of the limb-specific plasmid DNAs hybridized detectably with the tube ^{32}P-nuclear RNA. By contrast, Figures 12A and 12B show that the TP22 DNA hybridized about equally with the limb and tube ^{32}P-nuclear RNAs. Together, these transcription data correspond directly with results obtained with corolla limb and tube mRNAs (Figures 3A, 7C, and 7D, and Table 2) and indicate that the limb specificity of the petal mRNAs is controlled primarily at the transcriptional level.

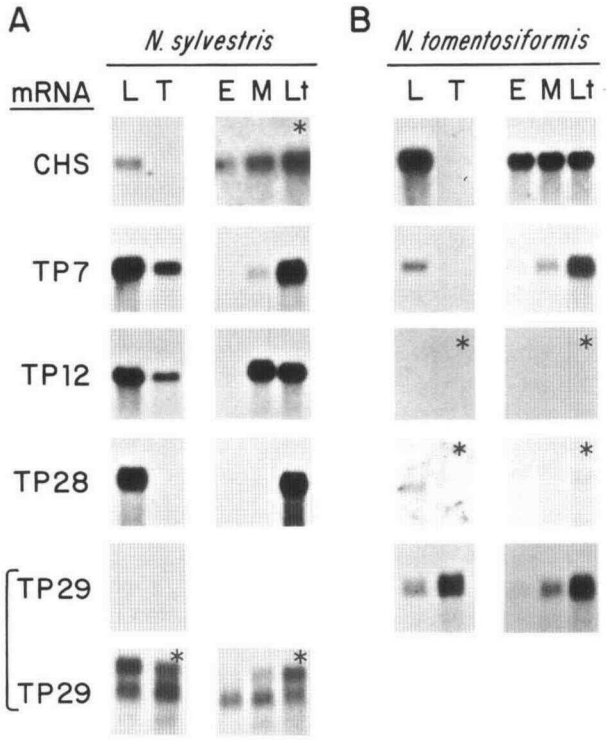

Figure 11. Representation of Petal mRNAs in the Corollas of Tobacco Progenitor Species.

Polysomal poly(A) mRNAs were isolated from corolla limb (L) and tube (T) regions (Figures 1C and 1D) and from whole corollas (tube plus limb) at early (E), middle (M), and late (Lt) stages of flower development (bracketed stages, Figures 1C and 1D). The mRNAs were size-fractionated by electrophoresis on denaturing agarose gels, transferred to nytran, and hybridized with labeled plasmid DNA probes, as outlined in Methods. Gel blots marked with asterisks were exposed for long periods of time (1 to 3 days). Other lanes were exposed for 0.5 to 7 hr, depending upon the probe. CHS, chalcone synthase.

(A) Representation of tobacco petal mRNAs in *N. sylvestris* corolla regions and developmental stages. Limb and tube gel blot lanes contained 0.4 μg of stage 12 mRNA. Temporal gel blots contained 1 μg of mRNA from corollas at the designated stages (Figure 1C).

(B) Representation of tobacco petal mRNAs in *N. tomentosiformis* corolla regions and developmental stage. Limb and tube gel blot lanes contained 0.4 μg of stage 12 mRNA. Temporal gel blots contained 1 μg of mRNA from corollas at the designated stages (Figure 1D).

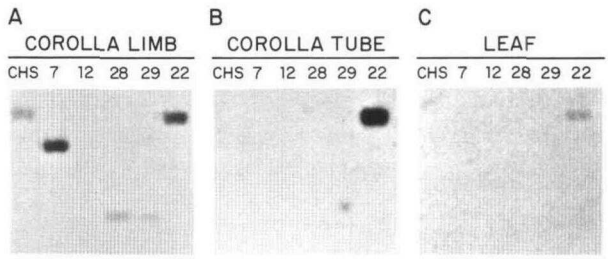

Figure 12. Hybridization of Petal Plasmid DNAs with ^{32}P-nuclear RNAs.

Plasmid DNAs were digested with PstI, size-fractionated by electrophoresis to separate plant DNA inserts from vector DNA, transferred to nytran, and hybridized with ^{32}P-nuclear RNAs synthesized in vitro, as outlined in Methods.

(A) Hybridization of plasmid DNAs with ^{32}P-nuclear RNA from the limb region of stage 12 corollas (Figure 1A). CHS, chalcone synthase.

(B) Hybridization of plasmid DNAs with ^{32}P-nuclear RNA from the tube region of stage 12 corollas (Figure 1A).

(C) Hybridization of plasmid DNAs with leaf ^{32}P-nuclear RNA.

Organ Specificity

We hybridized gel blots containing representative petal plasmid DNAs (CHS, TP7, TP12, TP22, TP28, TP29) with leaf ^{32}P-nuclear RNA to determine whether the petal-specific gene expression patterns were controlled transcriptionally. Figure 12C shows that none of the limb-specific plasmid DNAs (CHS, TP7, TP12, TP28, TP29) produced a detectable hybridization signal with leaf ^{32}P-nuclear RNA. This result is consistent with the nondetectable, or highly reduced, signals obtained with leaf mRNA using these plasmid probes (Figure 3B and Table 3). By contrast, Figure 12C shows that the TP22 plasmid produced a signal with leaf ^{32}P-nuclear RNA. This signal, however, was lower than those obtained with corolla limb and tube ^{32}P-nuclear RNAs (Figures 12A and 12B) and correlated directly with the reduced TP22 mRNA prevalence in the leaf (Figure 3B). Together, these data indicate that the organ specificity of the petal mRNAs is controlled primarily by transcriptional processes.

Cell Specificity

We constructed chimeric chalcone synthase/GUS and TP12 patatin/GUS genes and then transferred these genes to tobacco to determine whether the cell-specific expression patterns observed within the corolla limb region (Figures 5 to 7) were regulated transcriptionally (see Methods). Figure 13A shows that intense blue color resulting from GUS enzyme activity was visualized within the adaxial (AdE) and abaxial (AbE) epidermal layers of stage 12 petal tip regions containing the chalcone synthase/GUS gene. GUS activity was either nondetectable or present at much lower levels in limb mesophyll cells (Figure 13A). In addition, GUS activity was highly reduced in tube epidermal cells (data not shown). These data reflect those obtained with the mRNA localization experiments (Figures 5C and 7C) and indicate that the chalcone synthase limb-epidermal–specific gene expression pattern is controlled, to a first approximation, at the transcriptional level.

By contrast, Figure 13B shows that a stage 8 petal tip region from a plant containing the TP12 patatin/GUS gene produced a strong blue color within the mesophyll as well as within both epidermal cell layers. GUS activity levels were reduced significantly in both of these cell types within the tube region (data not shown). This result correlates directly with the limb specificity of the TP12 patatin mRNA (Figures 3A and 7D) and indicates that the TP12 limb-specific gene expression pattern is controlled at the transcriptional level, like other limb-specific genes (Figures 12A and 12B). On the other hand, localization of GUS activity with limb mesophyll *and* epidermal cells differed significantly from the mesophyll-specific TP12 mRNA localization pattern obtained with the in situ hybridization studies (Figures 5F, 6H to 6J, and 7D).

There are two possible explanations for this disparity. One is technical and the other is conceptual. Because GUS is a relatively stable enzyme (Jefferson et al., 1987), its activity within stage 8 limb epidermal cells might be a reflection of TP12 promoter activity in epidermal cells at an earlier stage of corolla development. If so, then the TP12 promoter might actually be inactive, or active at a reduced level, within limb epidermal cells at stage 8 and the TP12 mesophyll-specific mRNA pattern would reflect this transcriptional inactivity. Alternatively, GUS activity within the epidermal and mesophyll cells might be due to TP12 promoter activity in both of these limb cell types at stage 8. If so, then the striking difference in TP12 mRNA accumulation levels within the mesophyll and epidermis would be caused by post-transcriptional events, such as selective mRNA turnover in the epidermal layers. We cannot distinguish between these possibilities at the present time because of the nature of the GUS reporter system and our inability to measure cell-specific transcription events in situ. Nevertheless, the results obtained with the chimeric chalcone synthase/GUS and TP12 patatin/GUS genes (Figure 13) indicate that transcriptional processes are, in part, responsible for generating the epidermal- and mesophyll-specific expression patterns, and that post-transcriptional processes may contribute to the generation of the mesophyll-specific pattern as well. Taken together, the runoff transcription experiments (Figure 12) and GUS reporter gene studies (Figure 13) indicate that the petal gene organ, region, and cell specificities are controlled primarily at the transcriptional level.

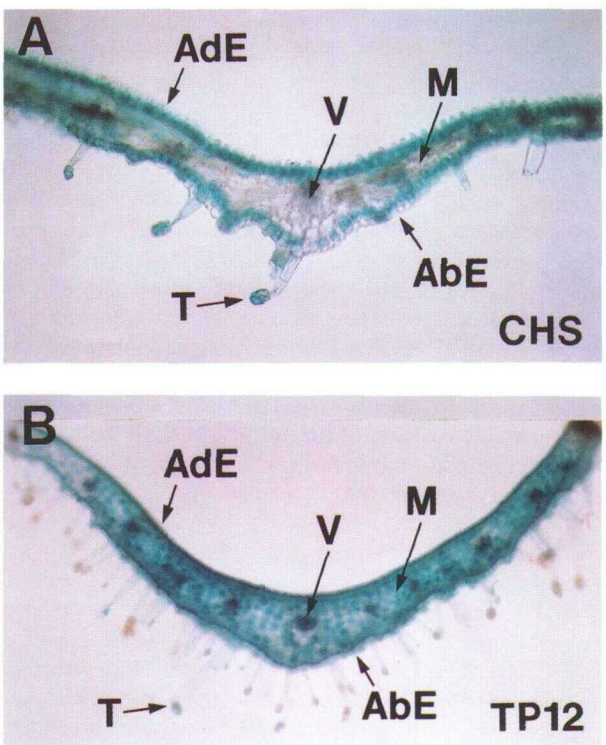

Figure 13. Visualization of GUS Activity within Corolla Limb Cell Types.

DNA fragments containing 5′ chalcone synthase and TP12 patatin gene regions were fused with the *E. coli* GUS gene and transferred to tobacco plants, as outlined in Methods. Freehand sections (100 μm) of corolla limb regions equivalent to those used for the mRNA localization studies (Figures 5 to 7) were assayed for GUS enzyme activity, as outlined in Methods. AbE, AdE, M, V, and T represent abaxial epidermis, adaxial epidermis, mesophyll, vascular bundle, and trichome, respectively.
(A) Localization of GUS enzyme activity within stage 12 corolla limb cell types of a chalcone synthase/GUS transformant.
(B) Localization of GUS enzyme activity within stage 8 corolla limb cell types of a TP12 patatin/GUS transformant.

DISCUSSION

A High Degree of Overlap Exists between Prevalent Corolla Limb and Tube mRNA Sets

We investigated the gene expression patterns that occur during tobacco corolla development. We identified two distinct classes of prevalent mRNAs in stage 12 corollas. At this developmental stage, the corolla contains a mature, open limb

that is pink due to the epidermal-specific accumulation of anthocyanin, and a cream-white tube that lacks epidermal layer anthocyanin and papillae (Figures 1A, 1B, 6A, and 7A). One mRNA class, represented by TP22, is present at approximately equal levels in both limb and tube regions (Figure 3A and Table 2). The other class, which includes the chalcone synthase, TP7 isoflavone reductase, TP12 patatin, TP13, TP20, TP28, and TP29 mRNAs, is also present in the limb and tube, but accumulates to a higher level in the limb (Figure 3A and Table 2). No mRNAs were found in our screens (see Methods) that are present exclusively, or at elevated levels, in the tube region. We conclude from these results that, at least with respect to prevalent-class petal mRNAs, there is a significant overlap between the diverse mRNA sequences present in stage 12 corolla limb and tube regions, and that several different mRNAs accumulate preferentially in a limb-specific manner during corolla development (Figures 3A and 4).

Petal mRNAs Are Present in Other Organ Systems

Previously, we showed that a stage 12 corolla contains approximately 25,000 diverse mRNAs (Kamalay and Goldberg, 1980). The vast majority (>97%) of these mRNAs are rare-class sequences constituting only about 10^{-3}% each when averaged over the petal as a whole (Goldberg et al., 1978; Kamalay and Goldberg, 1980). Although many of these mRNAs could be more prevalent in minor corolla cell types (e.g., trichomes, stomata), most are 1000- to 10,000-fold lower in prevalence than the petal mRNAs obtained in our screens (Table 2), or other prevalent-class corolla mRNAs (Goldberg et al., 1978; Kamalay and Goldberg, 1980), and would not have been detected in the experiments described here. Comparisons between the rare class mRNA sets of different tobacco organ systems indicated that, within the sensitivity of our hybridization procedure (±300 diverse mRNAs), the corolla and leaf mRNA sequence sets are qualitatively identical to each other, and that approximately 6000 diverse rare mRNAs are petal/leaf–specific and are not detectable in other organ system mRNA populations (Kamalay and Goldberg, 1980). This finding is consistent with the similar cell types, tissue organization patterns, and developmental programs of petals and leaves (Esau, 1977).

All of the prevalent petal mRNAs that we investigated have homologs, or highly related counterparts, in at least one heterologous floral or vegetative organ system (Figure 3B and Table 3). In most cases, the petal mRNAs are present in heterologous organs at levels 20- to 1000-fold lower than those observed in the corolla as a whole (e.g., TP7 pistil mRNA; Table 3), although in some organs their prevalences approach, or slightly exceed, those in the corolla (e.g., TP13 stem mRNA; Table 3). All of the limb-specific mRNAs, however, have their highest levels within the corolla limb region, irrespective of their representation in other organ systems (Tables 2 and 3). These results indicate that the prevalent-class petal mRNAs are not petal specific in the strictest sense; they are only present in the petal at elevated levels relative to other organs. This differs significantly from the situation that we observed in the anther, in which a large number of prevalent-class mRNAs are present exclusively within the anther and are not detectable in other organ systems, including the petal (Koltunow et al., 1990).

The cell localization patterns of petal mRNAs in other organs are different from those observed within the corolla (Figures 5 to 9). For example, the TP7 isoflavone reductase mRNA is highly concentrated within stem-differentiating xylem cells (Figure 8). Although the TP7 mRNA represents only about 0.1% of the stem mRNA mass as a whole (Tables 2 and 3), we estimate that its prevalence is at least 50-fold higher in this stem cell type. By contrast, the TP7 mRNA is localized preferentially within the corolla epidermal layers and is not detectably present within the xylem of the midvein or other vascular bundles (Figures 5 and 6). Because there are several TP7-related DNA sequences in the tobacco genome (Figure 10), we cannot state with certainty whether the same gene is active within the corolla and stem. This is a fairly reasonable assumption, however, because the two tobacco DNA gel blot fragments that hybridize most strongly with the TP7 cDNA contain related TP7 genes that were inherited from *N. sylvestris* and *N. tomentosiformis* (Figure 10) and both are active in the corolla (Figure 11; G. N. Drews and R. B. Goldberg, unpublished results). We conclude from these data, and those obtained with the chalcone synthase and TP12 patatin mRNAs (Figure 9), that petal genes can be expressed in developmentally distinct cell types in heterologous organ systems.

Most of the petal mRNAs studied, including representatives from both the limb-specific (CHS, TP7, TP13, TP20, TP29) and limb/tube (TP22) mRNA classes, are present in the leaf at levels ranging from almost 100% of that observed in the corolla to 1000-fold reduced in prevalence (Figure 3B and Table 3). The runoff transcription studies presented in Figure 12 show that the reduced levels of petal mRNAs within the leaf correlate with reduced rates of transcription in this organ system. We conclude from these observations that significant quantitative differences can occur between mRNAs shared by the petal and other organs, and that the organ specificity of genes encoding prevalent petal mRNAs is controlled, at least with respect to the leaf, primarily at the transcriptional level.

Several Functionally Unrelated mRNAs Are Present in the Corolla Limb-Specific Set

Most of the petal mRNAs that we studied are limb specific (Figure 3A and Table 2). One of these, chalcone synthase, encodes an important enzyme of the flavonoid biosynthesis pathway that leads to the formation of anthocyanin and other flavonol compounds important for insect attraction, UV light protection, and defense (Hahlbrock and Grisebach, 1979). We expected that the chalcone synthase mRNA would be limb specific in tobacco because of its pink/white coloration pattern (Figure 1A) and because of the work of others (Koes et al., 1990; Schmid

et al., 1990; Fritze et al., 1991). Consequently, we utilized this mRNA as a reference point for our petal mRNA studies.

We sequenced four of the six other limb-specific mRNAs studied here (Figure 3A and Table 2) and found that two of them, TP28 and TP29, did not produce a statistically significant match with any known mRNA or protein, including those of the anthocyanin biosynthetic pathway (Martin et al., 1991). We were surprised, however, to find that the TP7 and TP12 mRNAs encoded proteins related to isoflavone reductase (Paiva et al., 1991) and patatin (Bevan et al., 1986), respectively. As shown in Table 2, these mRNAs are the most prevalent petal mRNAs identified in our screens, collectively constituting almost 5% of the limb mRNA when averaged over the entire limb (Table 2), and even higher on a cell-type–specific basis (Figure 5). These proteins are not part of the anthocyanin biosynthetic pathway (Martin et al., 1991), nor do they play any apparent role in anthocyanin deposition within the limb region.

What function could the isoflavone reductase and patatin proteins perform in the corolla and within the limb region in particular? Isoflavone reductase is an important enzyme of the isoflavone phytoalexin pathway in legumes (Paiva et al., 1991) and, as such, appears to play a major role in defense responses. Although tobacco has not been shown to utilize flavonoid- and isoflavonoid-like phytoalexins in its response to fungal attack (Dixon et al., 1983), it is possible that isoflavonoids are used in this capacity within the limb during flower opening. This role would be consistent with the high expression level of the TP7 isoflavone reductase gene in stem xylem cells (Figure 8). Patatin, on the other hand, is the major storage protein of potato tubers and is utilized as a food source for this organ (Bevan et al., 1986). Patatin also has, however, acyl hydrolase activity (Rosahl et al., 1987; Andrews et al., 1988), which is thought to play a role in sesquiterpenoid phytoalexin induction in solanaceous plants by releasing fatty acid elicitors (Stermer and Bostock, 1987; Vancanneyt et al., 1989). Recently, the osmotin gene has also been shown to be limb specific in tobacco stage 12 corollas (Kononowicz et al., 1992). Osmotin has antifungal activity and appears to play a role in defense responses as well (Woloshuk et al., 1991). Thus, at least two types of limb-specific mRNAs exist—those involved in flavonoid biosynthesis, such as chalcone synthase and EPSP synthase (Benfey and Chua, 1989), and those, such as isoflavone reductase, patatin, and osmotin, which might play a defensive, or stress-related role, within the corolla. Each class has been recruited during the course of evolution into regulatory networks that control gene expression within the limb, but for different biological purposes.

Limb-Specific Gene Expression Is Unaffected by Corolla Coloration Pattern

Tobacco originated as an allotetraploid hybrid from a cross between the diploid species *N. sylvestris* and *N. tomentosiformis* (Goodspeed, 1954; Gray et al., 1974; Okamuro and Goldberg, 1985). Comparisons between the single-copy DNAs of tobacco and its progenitor species suggested that this was a recent event occurring only a few million years ago (Okamuro and Goldberg, 1985). Tobacco has a pink/white corolla coloration pattern that resembles that of *N. tomentosiformis*, in contrast to the unpigmented, chalk-white corolla of *N. sylvestris* (Figure 1). This indicates that the presence of anthocyanin within the *N. tomentosiformis* corolla is a dominant characteristic.

What accounts for the absence of pigmentation (anthocyanin and chlorophyll) in the *N. sylvestris* corolla? Coloration patterns in tobacco species are controlled by several gene loci (Smith, 1937). Four genes, designated as *C*, *P*, *B1*, and *B2*, are involved in anthocyanin deposition, whereas another, called *G*, controls the presence of chlorophyll (Smith, 1937). Undoubtedly, other genes are also involved (Dooner and Robbins, 1991). The *C* gene appears to be analogous to the corn *R* gene (Ludwig and Wessler, 1990) because its absence selectively prevents anthocyanin accumulation in the corolla and stem in the presence of *P*, but not in the anthers and pollen (Smith, 1937). *B1* and *B2* control anthocyanin deposition within the anther (Smith, 1937) and they are probably *R*-type regulatory genes as well. The absence of chlorophyll within the *N. sylvestris* corolla is probably due to a defect in a gene analogous to *G*. On the other hand, the lack of anthocyanin could be due to a defect in either a structural gene like *P* or a regulatory gene like *C*. Because the chalcone synthase gene is expressed normally in *N. sylvestris* (Figure 11A), the simplest explanation for the absence of pigmentation within the *N. sylvestris* corolla is that it has a defect in a structural gene (*P*) specifying an enzyme of the anthocyanin pathway. The tobacco corolla probably has a pink limb due to the presence of *P* from *N. tomentosiformis*, and a cream-white tube with only a trace of green because of the dilution of *N. tomentosiformis G* genes with recessive *g* alleles from *N. sylvestris* (Figure 1).

Most of the limb-specific mRNAs, including chalcone synthase, TP7 isoflavone reductase, and TP12 patatin, are also limb specific in the corollas of *N. sylvestris* and *N. tomentosiformis*, when they are present at detectable levels (Figure 11). This result indicates that the tobacco limb-specific gene expression programs were inherited from both diploid progenitors and that limb specificity is correlated with the morphological division of the corolla into limb and tube regions, regardless of whether the limb is pigmented or not. *N. sylvestris* and *N. tomentosiformis* evolved from a common ancestor shortly after the emergence of flowering plants over 150 million years ago (Goodspeed, 1954; Okamuro and Goldberg, 1985). Thus, whatever genes control the regional specificity of the limb-specific mRNA set, these genes are probably of ancient origin and are connected ultimately to regulatory circuits responsible for establishing the limb and tube regions during corolla development, irrespective of the ultimate shape and coloration pattern of the corolla.

The TP29 Gene Has a Different Regional Specificity in Tobacco and *N. tomentosiformis* Corollas

The TP29 mRNA shows a remarkable difference between its regional specificity in tobacco and *N. tomentosiformis*—it is

limb specific in tobacco and tube specific in *N. tomentosiformis* (Figures 3A and 11B). The DNA and RNA gel blots presented in Figures 10 and 11 indicate that the TP29 gene was inherited from *N. tomentosiformis* and that only very divergent relatives are active in the *N. sylvestris* corolla. This implies that the same structural gene has undergone a change in its regional specificity since the time that *N. tomentosiformis* and *N. sylvestris* cross-pollinated to form the tobacco hybrid.

How could the regional specificity of the TP29 gene be altered? One possibility is that the *N. tomentosiformis* TP29 gene inherited by tobacco was limb specific, and that this gene has been modified in *N. tomentosiformis after* the hybridization event creating tobacco took place. Alternatively, the *N. tomentosiformis* TP29 gene inherited by tobacco was tube specific, and this gene either has been modified in tobacco *after* the hybridization event occurred or its expression has been altered by its presence in the tobacco allotetraploid nuclear environment. Because all of the other limb-specific mRNAs retain their regional specificities in both tobacco and the diploid progenitors (Figure 11), the simplest explanation is that the TP29 gene has undergone a structural modification in either tobacco or *N. tomentosiformis* since the time that tobacco was created. If so, then this modification probably involves DNA sequences that control region specificity, because the TP29 limb-specific gene expression program is controlled primarily at the transcriptional level (Figures 12A and 12B). Experiments with both TP29 gene homologs should distinguish between these possibilities and provide clues as to the DNA sequences involved in corolla region specificity.

Limb-Specific Genes Are Not Regulated Coordinately during Corolla Development

The limb-specific genes studied here are not regulated coordinately in the formal sense. First, each limb-specific mRNA has a different temporal accumulation pattern during corolla development (Figures 4A and 6). For example, the chalcone synthase mRNA accumulates relatively early, prior to corolla extension above the sepal tips (stage 3), whereas the TP28 mRNA accumulates very late during flower opening (stage 12). Second, each mRNA accumulates to a different level within the limb at stage 12, and the ratio of limb to tube mRNA prevalences differs for each mRNA and varies over a 25-fold range (Figure 3A and Table 2). For example, the TP12 patatin mRNA represents approximately 1% of the limb mRNA mass and is 125-fold more prevalent in the limb than the tube (Table 2). By contrast, the chalcone synthase and TP28 mRNAs represent only 0.2% of the limb mRNA mass each, and are only five times more prevalent in the limb than the tube (Table 2). Finally, limb-specific mRNAs accumulate to high levels within different corolla cell types (Figures 5 to 7). The chalcone synthase, TP7 isoflavone reductase, TP28, and TP29 mRNAs are epidermal specific, whereas the TP12 patatin mRNA is mesophyll specific (Figures 5 to 7). We conclude that the only expression pattern shared by all limb-specific genes is their regional specificity within the corolla.

Most aspects of the limb-specific gene expression programs are controlled by transcriptional processes, although post-transcriptional events probably contribute as well. First, regional specificity is controlled primarily at the transcriptional level because all limb-specific genes investigated are transcribed at a higher rate in the limb than the tube (Figures 12A, 12B, and 13). Second, mRNA levels within the limb at stage 12 are also controlled, in part, by transcriptional processes because in most cases mRNA prevalences correlate with relative gene transcription rates (e.g., TP7 vs TP29; Table 2 and Figure 12A). Post-transcriptional events probably also play a role because genes encoding mRNAs with similar limb prevalences (CHS, TP28, TP29; Table 2) have different transcriptional rates, and because the TP12 patatin gene is not transcribed detectably at the sensitivity level of our runoff experiments (Figure 12A), even though this mRNA is quite prevalent in the limb at stage 12 (Figure 3A and Table 2). Finally, limb cell specificity is generated, in part, at the transcriptional level because GUS activity was visualized specifically within limb epidermal cells of transformants containing the chalcone synthase/GUS gene (Figure 13A), and within the mesophyll cells of TP12 patatin/GUS transformants (Figure 13B). We cannot exclude, however, the possibility that post-transcriptional events also contribute to establishing the mesophyll-specific gene expression pattern, because GUS activity was visualized within the limb epidermal cells of TP12 patatin/GUS transformants (Figure 13B), even though TP12 mRNA was not observed in these cells at the sensitivity level of our in situ hybridization procedure (Figures 5 to 7). Collectively, these results suggest that a common set of transcription factors is responsible for generating the regional specificity of all limb-specific genes within the corolla. By contrast, different factors control individual transcriptional rates and are responsible for generating distinct temporal and cellular expression programs. We predict from this model that combinations of diverse *cis* elements and transcriptional factors operate during corolla development to generate a unique expression pattern for each limb-specific gene.

What could be responsible for controlling the regional specificity of the limb-specific mRNA set? Over 50 years ago, a duplicate pair of tobacco genes, designated as *E1* and *E2*, were found to control coloration pattern in the dark red corolla of *N. sanderae* (Smith, 1937), one of the few *Nicotiana* species with an all-red corolla limb and tube (Goodspeed, 1954). Absence of both genes blocks pigment deposition on the abaxial side of the limb and prevents extension of pigment to the tube region (Smith, 1937). This results in a red/white coloration pattern analogous to that observed in tobacco (Figure 1A) and in the *delila* mutant of *Antirrhinum* (Almeida et al., 1989; Martin et al., 1991; Jackson et al., 1992). It is possible that the limb-specific gene expression patterns observed in all three tobacco species are caused by the absence of an *E1*- or *E2*-like allele, and that the *E* genes are involved in the transcriptional regulation of the limb-specific gene set within the tube, analogous to how the *delila* transcriptional regulatory gene is thought to function in *Antirrhinum* (Martin et al., 1991; Goodrich et al., 1992; Jackson et al., 1992). Other transcription factors, working independently of the putative *E*-like factors, would be

responsible for transcription within the limb. If this model is correct, then we predict that the tobacco limb-specific genes studied here should be expressed at equal levels within the limb and tube of the *N. sanderae* corolla, and that *N. sanderae* might prove very useful for isolating tobacco regulatory genes that are involved in generating corolla-region–specific gene expression patterns.

How Does the Limb/Tube Morphological Pattern Get Established during Corolla Development?

Regardless of the precise details of how limb-specific genes are transcriptionally regulated during corolla development, these genes are far removed from those involved in corolla region and cell specification processes, and their transcriptional machinery must respond to signals set in motion by upstream regulatory networks that ultimately control the morphological division of the corolla into limb and tube regions. Figure 2 shows that fusion of the five tobacco petal primordia occurs very early in development, at about the time that vascular cell differentiation processes are being completed (stage −5). How the lateral margins of the petal primordia recognize and fuse with one another remains a major, unanswered question. Nevertheless, the fusion zone between the petal primordia created by this process becomes the tube region and the unfused apices are destined ultimately to become the limb (Figure 2). Thus, the partitioning of the corolla into the limb and tube regions occurs very early in petal development and is thought to be controlled by divisions within different meristems (Nishino, 1978). This is consistent with the localization of the chalcone synthase mRNA within the upper corolla region at stage 3 prior to limb maturation (Figure 4). Because the cells in both corolla regions are derived, ultimately, from the same primordial L1, L2, and L3 cell layers (Satina, 1944), positional information within the floral meristem must be acting on the petal primordia to set the separate developmental fates of limb and tube regions. Clearly, what genes control the morphological differentiation of the corolla into limb and tube and how these pattern-forming genes are connected to regulatory circuits that control the regional specificity of genes expressed within the corolla later in development remain to be determined.

METHODS

Growth of Plants

Tobacco plants (*Nicotiana tabacum* cv Samsun) and progenitor species (*N. sylvestris* and *N. tomentosiformis*) were grown in the greenhouse as described by Kamalay and Goldberg (1980). A description of tobacco flower development was published previously (Koltunow et al., 1990). Developmental characteristics of organ systems used for RNA preparation were described by Kamalay and Goldberg (1980) and Cox and Goldberg (1988).

Polysomal mRNA Isolation

Polysomal poly(A) mRNAs were isolated according to Cox and Goldberg (1988).

DNA Isolation and Labeling

DNAs were isolated as described by Jofuku and Goldberg (1988). DNAs were labeled by nick-translation under conditions specified by Bethesda Research Laboratories.

Gel and Dot Blot Studies

DNA and RNA gel blot studies and RNA dot blot experiments were carried out as described by Koltunow et al. (1990).

Light Microscopy of Petal and Corolla Sections

Corollas were dissected from flower buds at the relevant developmental stages and either sectioned freehand with a razor blade or fixed with glutaraldehyde as described by Cox and Goldberg (1988). Fixed corollas were embedded in paraffin, sliced into 10-μm sections, and stained with 0.05% toluidine blue as outlined by Cox and Goldberg (1988). Stained and freehand sections were photographed with bright-field illumination as described by Koltunow et al. (1990).

In Situ Hybridization Studies

In situ hybridization studies with paraffin-embedded organ system sections were carried out as described by Cox and Goldberg (1988) and Perez-Grau and Goldberg (1989).

Synthesis of Single-Stranded RNA Probes

Labeled ^{35}S-RNAs were synthesized using the pGEM transcription system under conditions specified by Promega Biotec.

Runoff Transcription Studies

Synthesis of ^{32}P-RNA in isolated nuclei was carried out as described by Walling et al. (1986) and Cox and Goldberg (1988).

Construction and Screening of Petal cDNA Libraries

Stage 12 tobacco corolla limb and tube cDNA libraries were constructed in pBR329 (Covarrubias and Bolivar, 1982) as outlined by Koltunow et al. (1990). Approximately 13,000 and 8000 limb and tube cDNA clones were obtained, respectively. Petal-specific cDNA clones representing mRNAs present exclusively, or at elevated levels, in each corolla region were identified by screening replica plates of each library with limb ^{32}P-cDNA, tube ^{32}P-cDNA, leaf ^{32}P-cDNA, and a mixture of root, stem, pistil (stage 6), and anther (stage 6) ^{32}P-cDNAs as described by Koltunow et al. (1990).

Screening of Tobacco Genome Library

A λTP12 genomic clone was isolated from a λCharon 32 leaf DNA library (Koltunow et al., 1990) by the plaque hybridization procedures outlined in Jofuku and Goldberg (1988). A chalcone synthase genomic clone, designated as λCS2, was identified in this library by cross-hybridization with a parsley chalcone synthase cDNA clone (pLF15) kindly provided by Professor Klaus Hahlbrock (Reimold et al., 1983). A 2-kb XbaI fragment from this genomic clone, designated as pCS2X2.0, was used for the gel blot and in situ hybridization experiments. This clone contained chalcone synthase coding sequences (G. N. Drews and R. B. Goldberg, unpublished results).

Scanning Electron Microscopy

Scanning electron microscopy was carried out as described by Koltunow et al. (1990).

Histochemical Assay for β-Glucuronidase Enzyme Activity

Histochemical staining for β-glucuronidase (GUS) activity was carried out according to the procedure of Jefferson et al. (1987) with minor modifications to optimize visual detection of GUS activity in petals (Kosugi et al., 1990; Martin et al., 1992). In brief, petals were sliced freehand into 100-μm sections and placed in 0.05 M sodium phosphate buffer (pH 7.0) containing 0.0005 M ferrocyanide, 0.5% Triton X-100, 0.001 M EDTA, 0.05 M ascorbate, 10% methanol, and 0.001 M 5-bromo-4-chloro-3-indolylglucuronide (X-gluc). Following vacuum infiltration, GUS reactions were carried out at 37°C. After a visible blue histochemical reaction occurred, the petals were fixed, cleared of pigments, and photographed as described previously (Koltunow et al., 1990).

Construction of Chimeric Genes and Transformation Studies

NcoI sites were generated at the TP12 and chalcone synthase gene translation start sites using the T7-GEN in vitro mutagenesis kit as specified by United States Biochemical Corp. Chimeric TP12/GUS and chalcone synthase (CHS)/GUS genes were constructed by fusing 2-kb 5′ TP12 and 1.3-kb 5′ chalcone synthase gene fragments with the *Escherichia coli* GUS gene (Jefferson et al., 1987) at their NcoI sites. The chimeric TP12/GUS and CHS/GUS genes were transferred to tobacco as outlined in Koltunow et al. (1990).

ACKNOWLEDGMENTS

We thank our colleagues Jessie Truettner, Kathleen Cox, Robert Fischer, Tom Sims, Linda Walling, John Harada, Diane Jofuku, Jack Okamuro, Ramin Yadegari, Paul Sanders, Genaro de Paiva, and Anna Koltunow for advice, help, and stimulating discussions during the course of this work. We also thank Annette Salinger and Sharon Hue Tu for assistance with the in situ hybridization and histological experiments, and Jef Seurinck of Plant Genetic Systems for sequencing a TP7 genomic clone. G.N.D. and T.P.B. were supported by a McKnight Foundation Predoctoral Fellowship and a National Institutes of Health Postdoctoral Fellowship, respectively. This research was supported by a National Science Foundation grant to R.B.G.

Received September 21, 1992; accepted September 30, 1992.

REFERENCES

Almeida, J., Carpenter, R., Robbins, T.P., Martin, C., and Coen, E. (1989). Genetic interactions underlying flower color patterns in *Antirrhinum majus*. Genes Dev. **3,** 1758–1767.

Andrews, D.L., Beames, B., Summers, M.D., and Park, W.D. (1988). Characterization of lipid acyl hydrolase activity of the major potato tuber protein patatin by cloning and abundant expression in a baculovirus vector. Biochem. J. **252,** 199–206.

Benfey, P.N., and Chua, N.-H. (1989). Regulated genes in transgenic plants. Science **244,** 174–181.

Bevan, M., Barker, R., Goldsbrough, A., Jarvis, M., Kavanagh, T., and Itturriaga, G. (1986). The structure and transcription start site of the major potato tuber gene. Nucl. Acids Res. **14,** 4625–4638.

Coen, E.S. (1991). The role of homeotic genes in flower development and evolution. Annu. Rev. Plant Physiol. Plant Mol. Biol. **42,** 241–279.

Coen, E.S., and Meyerowitz, E.M. (1991). The war of the whorls: Genetic interactions controlling flower development. Nature **353,** 31–37.

Covarrubias, L., and Bolivar, F. (1982). Construction and characterization of new cloning vehicles VI. Plasmid pBR329, a new derivative of pBR328 lacking the 428 base pair inverted duplication. Gene **17,** 79–89.

Cox, K.H., and Goldberg, R.B. (1988). Analysis of plant gene expression. In Plant Molecular Biology: A Practical Approach, C.H. Shaw, ed (Oxford: IRL Press), pp. 1–34.

Dixon, R.A., Dey, P.M., and Lamb, C.J. (1983). Phytoalexin enzymology and molecular biology. Adv. Enzymol. **55,** 1–136.

Dooner, H.K., and Robbins, T.P. (1991). Genetic and developmental control of anthocyanin biosynthesis. Annu. Rev. Genet. **25,** 173–199.

Drews, G.N., and Goldberg, R.B. (1989). Genetic control of flower development. Trends Genet. **5,** 256–261.

Esau, K. (1977). Anatomy of Seed Plants (New York: John Wiley).

Fritze, K., Staiger, D., Czaja, I., Walden, R., Schell, J., and Wing, D. (1991). Developmental and UV light regulation of the snapdragon chalcone synthase promoter. Plant Cell **3,** 893–905.

Goldberg, R.B. (1988). Plants: Novel developmental processes. Science **240,** 1460–1467.

Goldberg, R.B., Hoschek, G., Kamalay, J.C., and Timberlake, W.E. (1978). Sequence complexity of nuclear and polysomal RNA in leaves of the tobacco plant. Cell **14,** 123–131.

Goodrich, J., Carpenter, R., and Coen, E.S. (1992). A common gene regulates pigmentation pattern in diverse plant species. Cell **68,** 955–964.

Goodspeed, T.H. (1954). The Genus *Nicotiana*: Origins, Relationships, and Evolution of its Species in Light of Their Distribution, Morphology, and Cytogenetics (Waltham, MA: Chronica Botanica).

Gray, J.C., Kung, S.D., Wildman, S.G., and Sheen, S.J. (1974). Origin of *Nicotiana tabacum* detected by polypeptide composition of fraction 1 protein. Nature **252,** 226–227.

Hahlbrock, K., and Grisebach, H. (1979). Enzymatic controls in the biosynthesis of lignin and flavonoids. Annu. Rev. Plant Physiol. **30,** 105–130.

Hicks, G.S. (1973). Initiation of floral organs in *Nicotiana tabacum*. Can. J. Bot. **51**, 1611–1617.

Jackson, D., Roberts, K., and Martin, C. (1992). Temporal and spatial control of expression of anthocyanin biosynthetic genes in developing flowers of *Antirrhinum majus*. Plant J. **2**, 425–434.

Jefferson, R.A., Kavanagh, T.A., and Bevan, M.W. (1987). GUS fusions: β-Glucuronidase is a sensitive and versatile fusion marker in higher plants. EMBO J. **6**, 3901–3907.

Jofuku, K.D., and Goldberg, R.B. (1988). Analysis of plant gene structure. In Plant Molecular Biology: A Practical Approach, C.H. Shaw, ed (Oxford: IRL Press), pp. 37–66.

Kamalay, J.C., and Goldberg, R.B. (1980). Regulation of structural gene expression in tobacco. Cell **19**, 935–946.

Kamalay, J.C., and Goldberg, R.B. (1984). Organ-specific nuclear RNAs in tobacco. Proc. Natl. Acad. Sci. USA **81**, 2801–2805.

Koes, R.E., van Blockland, R., Quattrocchio, F., van Tunen, A.J., and Mol, J.N.M. (1990). Chalcone synthase promoters in petunia are active in pigmented and unpigmented cell types. Plant Cell **2**, 379–392.

Koltunow, A.M., Truettner, J., Cox, K.H., Wallroth, M., and Goldberg, R.B. (1990). Different temporal and spatial gene expression patterns occur during anther development. Plant Cell **2**, 1201–1224.

Kononowicz, A.K., Nelson, D.E., Singh, N.K., Hasegawa, P.M., and Bressan, R.A. (1992). Regulation of the osmotin gene promoter. Plant Cell **4**, 513–524.

Kosugi, S., Ohashi, Y., Nakajima, K., and Arai, Y. (1990). An improved assay for β-glucuronidase in transformed cells: Methanol almost completely suppresses a putative endogenous β-glucuronidase activity. Plant Sci. **70**, 133–140.

Ludwig, S.R. and Wessler, S.R. (1990). Maize *R* gene family: Tissue-specific helix-loop-helix proteins. Cell **62**, 849–851.

Martin C., Prescott, A., Mackay, S., Bartlett, J., and Vrijlandt, E. (1991). Control of anthocyanin biosynthesis in flowers of *Antirrhinum majus*. Plant J. **1**, 37–49.

Martin, T., Wöhner, R.-V., Hummel, S., Willmitzer, L., and Frommer, W.B. (1992). The GUS reporter system as a tool to study plant gene expression. In GUS Protocols: Using the GUS Gene as a Reporter of Gene Expression, S.R. Gallagher, ed (New York: Academic Press), pp. 23–43.

Nishino, E. (1978). Corolla tube formation in four species of solanaceae. Bot. Mag. Tokyo **91**, 263–277.

Okamuro, J.K., and Goldberg, R.B. (1985). Tobacco single-copy DNA is highly homologous to sequences present in the genomes of its diploid progenitors. Mol. Gen. Genet. **198**, 290–298.

Paiva, N.L., Edwards, R., Sun, Y., Hrazdina, G., and Dixon, R.A. (1991). Stress responses in alfalfa 11. Molecular cloning and expression of alfalfa isoflavone reductase, a key enzyme of isoflavonoid phytoalexin biosynthesis. Plant Mol. Biol. **17**, 653–667.

Perez-Grau, L., and Goldberg, R.B. (1989). Soybean seed protein genes are regulated spatially during embryogenesis. Plant Cell **1**, 1095–1109.

Raven, P.H., Evert, R.F., and Eichhorn, S.E. (1986). Biology of Plants (New York: Worth).

Reimold, U., Kröger, M., Kreuzaler, F., and Hahlbrock, K. (1983). Coding and 3′ non-coding nucleotide sequence of chalcone synthase mRNA and assignment of amino acid sequence of the enzyme. EMBO J. **2**, 1801–1805.

Rosahl, S., Schell, J., and Willmitzer, L. (1987). Expression of a tuber-specific storage protein in transgenic tobacco plants: Demonstration of esterase activity. EMBO J. **6**, 1155–1159.

Satina, S. (1944). Periclinal chimeras in *Datura* in relation to development and structure of the style and stigma and calyx and corolla. Am. J. Bot. **31**, 493–502.

Schmid, J., Doerner, P.W., Clouse, S.D., Dixon, R.A., and Lamb, C.J. (1990). Developmental and environmental regulation of a bean chalcone synthase promoter in transgenic tobacco. Plant Cell **2**, 619–631.

Schwarz-Sommer, Z., Huijser, P., Nacken, W., Saedler, H., and Sommer, H. (1990). Genetic control of flower development by homeotic genes in *Antirrhinum majus*. Science **250**, 931–936.

Smith, H.H. (1937). Inheritance of corolla color in the cross of *Nicotiana langsdorfii* by *N. sanderae*. Genetics **22**, 347–360.

Smyth, D.R., Bowman, J.L., and Meyerowitz, E.M. (1990). Early flower development in *Arabidopsis*. Plant Cell **2**, 755–767.

Stermer, B.A., and Bostock, R.M. (1987). Involvement of 3-hydroxy-3-methylglutaryl coenzyme A reductase in the regulation of sesquiterpenoid phytoalexin synthesis in potato. Plant Physiol. **84**, 404–408.

Takatsuji, H., Mori, M., Benfey, P.N., Ren, L., and Chua N.-H. (1992). Characterization of a zinc finger DNA-binding protein expressed specifically in *Petunia* petals and seedlings. EMBO J. **11**, 241–249.

Vancanneyt, G., Sonnewald, U., Höfgen, R., and Willmitzer, L. (1989). Expression of a patatin-like protein in the anthers of potato and sweet pepper flowers. Plant Cell **1**, 533–540.

Walling, L., Drews, G.N., and Goldberg, R.B. (1986). Transcriptional and posttranscriptional regulation of soybean seed protein mRNA levels. Proc. Natl. Acad. Sci. USA **83**, 2123–2127.

Woloshuk, C.P., Meulenhoff, J.S., Sela-Buurlage, M., van den Elzen, P.J.M., and Cornelissen, B.J.C. (1991). Pathogen-induced proteins with inhibitory activity toward *Phytophthora infestans*. Plant Cell **3**, 619–628.